Role of Ceramide Accumulation in the Ventromedial Hypothalamus in Driving Systemic Metabolic Impairments During Obesity

By

Joshua A. Johnson

DISSERTATION

Presented to the Faculty of the Graduate School of Biomedical Sciences

The University of Texas Southwestern Medical Center at Dallas

In Partial Fulfillment of the Requirements

For the Degree of

DOCTOR OF PHILOSOPHY

The University of Texas Southwestern Medical Center at Dallas

Dallas, Texas

May 2019

DEDICATION

To my parents, Matt and Jonie Johnson

My brother, Michael

My wife, Michelle

My daughter, Erika

For in much wisdom is much vexation

Ecclesiastes 1:18, ESV

ACKNOWLEDGEMENTS

During my time in graduate school, I've been blessed to work with a number of individuals who are deserving of a number of superlatives. I hope this acknowledgement displays a small portion of the gratitude that you all deserve.

First, I want to thank my mentor, Dr. William Holland. Without your expertise, time, and mentorship, obviously none of this would be possible. Thanks for teaching me valuable skills, for allowing me the independence to try, fail, and generally make my own way in the lab without trying to make me simply an extension of your hands in the lab, with no input of my own. Although I know it's been painful sometimes, it's made me a better scientist and student, and for that, among many other things, I thank you. I also want to thank my dissertation committee members Joel Elmquist, Kevin Williams, and Jeff Zigman, who have all given me great feedback during our committee meetings. Special thanks also to Kevin Williams, whose lab completed the electrophysiology experiments for my thesis that gave such interesting results. I would also like to thank the NIH for sponsoring me with an F30 fellowship.

Further, I want to thank my colleagues in the Touchstone Diabetes Center, all of whom have been a major influence in my past four years. I first want to thank Tom Morley, a fellow MSTP student with whom I shared a lab bench. Tom was instrumental in getting me through the first year or so of grad school, with a ton of advice (both scientific and career-wise) along the way. Similarly, I want to thank Alex Ghaben, another fellow MSTP student who has been a great teacher of practical lab skills, and has always been a great sounding board for ideas. Another two students I want to mention are Chelsea Hepler and Mackenzie Pearson, both graduate students in the Touchstone Center; you both have been a joy to work with, and are always good for a smile and a word of encouragement.

I want to make a special effort to thank Ankit Sharma and Ezekiel Quittner-Strom, two techs in our lab. Although given the title of “technician”, we have a running joke in our lab that Ankit and Zeke are two of the best graduate students in the Touchstone Diabetes Center. I’ll never be able to thank the two of you enough for the technical assistance, words of encouragement, and emotional support that you’ve offered throughout the past few years. Another person who deserves special thanks is David Chen, an expert animal surgeon and technician in our lab. David’s supreme competence would be enough on its own to make him a valued member of the team; what doesn’t get noted often enough is his unbelievably positive attitude and cheerful demeanor.

Finally, I want to thank those closest to me. Mom and Dad, thanks for moving 1200 miles (give or take a few) to help support our family as I go through this MSTP program with a new baby. I’m not sure that it’s possible to thank you all for the sacrifice you’ve made to uproot your life and move to a new city. Michelle, my wife: thank you for everything. You’ve been a constant source of encouragement, love, and affection. Thanks for putting up with all the weekends in lab, particularly in the last few months of my graduate school work, and for being so understanding about the time commitments I’ve had away from you and Erika. You two have made me the luckiest man in the world. Lastly, thanks to my daughter, Erika, who has brought a joy into my life of a magnitude that I never thought possible.

Role of Ceramide Accumulation in the Ventromedial Hypothalamus in Driving Systemic Metabolic Impairments During Obesity

Joshua A. Johnson

The University of Texas Southwestern Medical Center at Dallas, 2017

William L. Holland, PhD

Obesity remains a tremendous national and global health epidemic and causes increased risk for any number of serious diseases. In the field of obesity, the idea of lipotoxicity (accumulation of toxic lipids in cells unable to handle them) has become an accepted concept, with increases in tissue lipids being recognized to cause tissue dysfunction during obesity. One of these lipotoxic lipids is ceramide, a sphingolipid. Ceramides have been demonstrated to blunt insulin sensitivity and contribute to numerous obesity-related impairments of tissue function, as seen in vascular endothelium, pancreatic islets, heart failure, and muscle, liver, and adipose insulin signaling. Recently, it has been shown that during obesity ceramides accumulate in the hypothalamus, the region of the brain known to regulate many aspects of metabolism. As hypothalamic lipid metabolism is rapidly being established as a key player in whole-body metabolic homeostasis, we became interested in whether this ceramide accumulation in the brain is another avenue via ceramide accumulation during obesity causes its numerous deleterious effects. To study this, we have overexpressed acid ceramidase in neurons in the ventromedial hypothalamus (VMH); this will decrease ceramide content specifically in this brain region vital to the control of glucose homeostasis and body weight. We found that ceramide accumulation in the VMH during obesity drives glucose intolerance without changing body weight or insulin sensitivity, and that this effect is due to an increase in glucagon sensitivity. Furthermore, we have included a general investigation on ceramide synthesis in response to high fat diet, as well as a blueprint for future studies of sphingolipid metabolism in the brain.

TABLE OF CONTENTS

PRIOR PUBLICATIONS

Joshua A Johnson, Sal Calo, Lekshmi Nair, Heidi B IglayReger, Megan Greenwald-Yarnell, Josh Skorupski, Martin G Myers, Peter F Bodary. 2012. Testosterone interacts with the feedback mechanisms engaged by Tyr985 of the leptin receptor and diet-induced obesity. ***The Journal of Steroid Biochemistry and Molecular Biology.***

Yi Zhu, Yong Gao, Caroline Tao, Mengle Shao, Shangang Zhao, Wei Huang, Ting Yao, Joshua A Johnson, Tiemin Liu, Aaron M Cypess, Olga Gupta, William L Holland, Rana K Gupta, David C Spray, Herbert B Tanowitz, Lei Cao, Matthew D Lynes, Yu-Hua Tseng, Joel K Elmquist, Kevin W Williams, Hua V Lin, Philipp E Scherer. 2016. Connexin 43 Mediates White Adipose Tissue Beiging by Facilitating the Propagation of Sympathetic Neuronal Signals. ***Cell Metabolism.***

William L Holland, Jonathan Y Xia, Joshua A Johnson, Kai Sun, Mackenzie J Pearson, Ankit X Sharma, Ezekiel Quittner-Strom, Trevor S Tippetts, Ruth Gordillo, Philipp E Scherer. 2017. Inducible Overexpression of Adiponectin Receptors Highlight the Roles of Adiponectin-Induced Ceramidase Signaling in Lipid and Glucose Homeostasis. ***Molecular Metabolism.***

Sachin Hajarnis, Ronak Lakhia, Matanel Yheskel, Darren Williams, Mehran Sorourian, Xueqing Liu, Karam Aboudehen, Shanrong Zhang, Kara Kersjes, Ryan Galasso, Jian Li, Vivek Kaimal, Steven Lockton, Scott Davis, Andrea Flaten, Joshua A Johnson, William L Holland, Christine M Kusminski, Philipp E Scherer, Peter C Harris, Marie Trudel, Darren P Wallace, Peter Igarashi, Edmund C Lee, John R Androsavich, Vishal Patel. 2017. microRNA-17 family promotes polycystic kidney disease progression through modulation of mitochondrial metabolism. ***Nature Communications.***

Caroline Tao, William L Holland, Qiong A Wang, Mengle Shao, Lin Jia, Kai Sun, Xiaoli Lin, YC Kuo, Joshua A Johnson, Ruth Gordillo, Joel K Elmquist, Philipp E Scherer. 2017. Short-Term vs. Long-Term Effects of Adipocyte Toll-like Receptor 4 Activation on Insulin Resistance in Male Mice. ***Endocrinology.***

LIST OF ABBREVIATIONS

AC	acid ceramidase
AgRP	agouti-related protein
CerS	ceramide synthase
CNS	central nervous system
CREB	cAMP response element-binding protein
dox	doxycycline
EPSC	excitatory post-synaptic current
FFA	free fatty acid
GCS	glucosylceramide synthase
GFP	green fluorescent protein
HFD	high fat diet
IPSC	inhibitory post-synaptic current
ITT	insulin tolerance test
LPL	lipoprotein lipase
OGTT	oral glucose tolerance test
PEPCK	phosphoenolpyruvate carboxykinase
PKCζ	atypical protein kinase C zeta
POMC	Proopiomelanocortin
RMP	resting membrane potential
rtTA	reverse tetracycline transactivator
S1P	sphingosine-1-phosphate
S1PR1	Sphingosine-1-phosphate receptor
SF1	steroidogenic factor 1
SPT	serine palmitoyltransferase
VMH	ventromedial hypothalamus
WT	wild type
β3-AR	beta3 adrenergic receptor

Chapter 1

Sphingolipids and body weight regulation – heading into the future

Introduction

Despite its recognition as a key driver of morbidity and mortality, obesity remains a major public health crisis, with greater than 1/3rd of adults in the United States being classified as obese[1, 2]. Obesity carries with it a number of comorbidities, vastly increasing the risk for related diseases like type 2 diabetes mellitus and cardiovascular disease[3, 4]. For many years, aberrant lipid accumulation outside of adipose tissue during obesity has been recognized as a driver of obesogenic morbidity and mortality, an effect termed "lipotoxicity" due to the toxic effects of lipid accumulation in tissues unadapted to their storage[reviewed in 5]. Efforts to isolate which lipid species are responsible for the destructive effects of hyperlipidemia have been successful in identifying sphingolipids and diacylglycerol as two broadly accepted mediators of insulin resistance and lipotoxicity[6].

A great deal of work has been done in recent years to characterize the effects of sphingolipid accumulation on insulin sensitivity and lipotoxic organ failure in any number of paradigms, with the general finding that accumulation of sphingolipids such as ceramide and glucosylceramide promote insulin resistance [reviewed in 7]. Sphingolipids are a ubiquitous lipid species found in cell and organelle membranes. They are created by a decarboxylation reaction of palmitoyl-CoA with serine, and the subsequent addition of a second, variable-length fatty acid chain, ultimately resulting in the production of ceramide. Ceramide is then able to be derivativized in a number of enzymatically-driven reactions, yielding *e.g.* ceramide-1-phosphate, sphingosine, glucosylceramide, or sphingomyelin. Although sphingolipids have been thoroughly studied in the context of type 2 diabetes mellitus and lipotoxic organ damage, comparatively less focus has been devoted to the study of sphingolipids and body weight regulation. We review below the effects of sphingolipids, and particularly ceramide on body weight

regulation in studies which directly modulate sphingolipid synthesis and disposal, with a focus on recent findings and future endeavors.

Whole body and peripheral sphingolipid metabolism perturbations

The sphingolipid synthesis pathway has a number of known pharmacologic modifiers, acting at various enzymatic steps in the pathway. Most notable in its usage, tolerability, and broad salutary effects has been myriocin, which inhibits the first, rate-limiting enzyme in the ceramide synthesis pathway, serine palmitoyltransferase[8]. Myriocin has been administered in a number of studies in animals undergoing high fat feeding, and results in consistent improvements in insulin sensitivity in a number of target tissues[9, 10]. Similarly, L-cycloserine (another inhibitor of serine palmitoyltransferase) and amitriptyline (an inhibitor of acid sphingomyelinase, which converts sphingomyelin into ceramide) both serve to reduce ceramide content and improve insulin sensitivity[9, 11, 12]. Importantly, blocking ceramide synthesis also improves body weight control: chronic whole-body treatment with inhibitors of ceramide synthesis during high fat feeding increases oxygen consumption [9, 12, 13], improves body composition [12, 14], decreases weight gain [11-13, 15], and increases activity [13], while seeming to have little effect on food intake [11-13]. These complementary effects point to the importance of ceramide synthesis and accumulation in promoting high fat diet-induced obesity.

Following its synthesis, ceramide can be further converted into a number of related metabolites. The attachment of sugar moieties by glucosylceramide synthase (GCS) results in glucosylceramides, which have been demonstrated to inhibit insulin sensitivity[7]. Although glucosylceramides are characterized to have a role in obesity-related insulin resistance, the data regarding GCS inhibitors and control of body weight and composition are mixed. Some reports demonstrate that oral pharmacologic GCS inhibitor treatment does not alter leptin

deficient, diet-induced, and chow-fed weight gain[16-19], while other reports have demonstrated that GCS inhibition strongly reduces body weight in both leptin deficient and lean settings [20-24]. However, it is important to note that the studies demonstrating body weight effects with GCS inhibition all occur with the GCS inhibitor AMP-DNM, while the studies showing no effect on body weight use various other inhibitors of GCS; it thus remains possible that AMP-DNM has some off-target effects not seen in the other inhibitors, causes toxicity-mediated weight loss, or that as-yet unknown subtleties exist in the modality of GCS inhibition between the various drugs.

Aside from pharmacologic interventions, some investigators have succeeded in genetically manipulating high fat fed animals to alter ceramide synthesis and degradation. One route of disrupting ceramide synthesis has been to knock out the rate-limiting enzymes of sphingolipid synthesis, serine palmitoyltransferase 1 & 2 (SPT1 & SPT2). A report demonstrated that knocking out SPT2 only in adipose tissue results in reduced HFD-induced weight gain and fat mass, due to increased adipose tissue browning and energy expenditure[12]. However, another group independently generated and studied adipose-specific SPT2 knockout animals; in this study, alterations in body weight with high fat feeding were not apparent, but a reduction in body fat mass remained, which was attributed to a severe lipodystrophy [25]. Similarly, another group has generated adipose-specific SPT1 knockout animals, which also demonstrate a lipodystrophic phenotype; alterations in body weight were not reported[26]. Finally**,** whole-body SPT2 haploinsufficient mice have been generated, and demonstrate reduced body weight gain when provided HFD, with no report of lipodystrophy[27].

Although SPT1/2 are rate-limiting and vital enzymes of sphingolipid synthesis, they do not confer any chain length specificity to the second fatty acid chain in the final ceramide product; this is done by the ceramide synthase enzymes, CerS1-6, which acylate sphinganine while each displaying preference for various chain length fatty acid chains[28]. Disruption of the ceramide synthases has been demonstrated by multiple groups with differing effects on metabolism depending on the site of deletion and ceramide synthase isoform. First, whole-body knockouts of ceramide synthase 6 (CerS6) show reduced body weight gain and body fat percentage on HFD, an effect attributed by the investigators to alterations in C:16 ceramide content [29]. Furthermore, deleting CerS6 specifically in brown adipose or liver improved body composition and HFD-induced weight gain, respectively [29]. Similarly, ceramide synthase 5 (CerS5) whole body knock-out animals have reduced body weight gain and improved insulin sensitivity on HFD, again occurring with substantial reductions of tissue C:16 and C:18 ceramides[30]. Conversely, haploinsufficiency of ceramide synthase 2 (CerS2) confers protection from HFD-induced insulin resistance, without altering body weight; CerS2 happloinsufficient animals did display a surprising *increase* in fat mass, despite their unchanged body weights[31]. This effect was attributed to compensatory increase in other ceramide synthases (CerS5 and CerS6), which (as shown above) drive deleterious effects on metabolism and weight gain.

After the acylation of sphinganine by a member of the CerS family, the final step in ceramide synthesis is a desaturation reaction carried out by dihydroceramide desaturase (Des1). Previously, members of our group have created Des1 knockout mice, which are born as unhealthy runts and ultimately die before 3 months of age with an abundance of abnormal

phenotypes[10]. Heterozygous Des1 knockout mice are grossly normal, but display increased adiposity and body weight on both chow and high fat diet despite improvements in insulin sensitivity[14]. The effects of Des1 in regards to ceramide metabolism are confounding, however; Des1 heterozygous animals were previously demonstrated to not have reduced tissue ceramide, although an increase in the ceramide:dihydroceramide ratio was reported, making any direct inferences of ceramide effects difficult[10].

Rather than knocking out enzymes of ceramide synthesis, some have deleted enzymes of ceramide depletion or modification. Sphingomyelin synthase converts ceramide into sphingomyelin, acting as a sink for cellular ceramide pools. Whole-body sphingomyelin synthase 2 (SMS2) knockout mice have been created; surprisingly, SMS2 knockouts have reduced body weight gain on HFD despite an increase in tissue ceramide, a finding attributed to decreased sphingomyelin content[27]. Ceramide kinase (CERK) converts ceramide into ceramide-1-phosphate, acting similar to SMS2 in its effects to decrease cellular ceramide pools. Whole-body CERK knockout mice have been reported, and demonstrate reduced body weight and adipose tissue inflammation on HFD[32].

Although others have chosen to genetically delete enzymes related to ceramide synthesis and degradation, our lab has utilized overexpression models to probe the effects of ceramide accumulation on body weight gain. Previously, we have overexpressed acid ceramidase or adiponectin receptors (which have intrinsic ceramidase activity[33-36]) targeted to white adipose, liver, muscle, macrophage, and brown adipose tissue with doxycycline-inducible genetic systems [37][35, 38][39][40]. Despite improvements in insulin sensitivity

resulting from reductions in tissue and serum ceramide, changes in body weight were not detected in any of these studies.

An aspect of sphingolipid studies that bears examination is the concept of ceramide trafficking between tissues. The study of this concept is quite complicated in practice, as tissue ceramide content can be affected by multiple factors: trafficking from distant tissues, systemic inflammation, and body weight changes. These confounding factors render many mouse models uninstructive. For instance, any tissue-specific mouse model causing changes in body weight are immediately confounding, as decreased body weight predicts decreased tissue ceramide. Similarly, manipulations which change tissue inflammation often come with a decrease in systemic inflammatory cytokines which are known drivers of ceramide synthesis. For instance, in our tissue-specific studies, we have noted that lowering ceramide content in adipose tissue can decrease ceramide accumulation in liver, and *vice versa*[35, 38]; however, these changes were seen in the context of reduced tissue inflammation, making a direct inference of ceramide trafficking difficult. It is known, however, that ceramide trafficking does occur and is important in the pathology of insulin resistance; low density lipoprotein binds ceramide in obesity, and exogenous treatment of animals with ceramide-laden lipoproteins causes insulin resistance[41].

Ceramides and central body weight regulation

From the studies reviewed above we conclude that ceramide accumulation during obesity is a causative factor in body weight gain; blocking ceramide synthesis through genetic or pharmacologic means results in reduced body weight in many experiments, with few

manipulations increasing body weight. Importantly, changes in body weight resulting from altered ceramide metabolism typically require whole-body pharmacologic or genetic manipulation. Tissue-targeted (*e.g.* liver, adipose tissue) alterations in sphingolipid content tend to alter only tissue insulin sensitivity without affecting body weight, with only one report of ceramide disruption in liver showing a minor reduction in body weight gain during HFD[29]. Conversely, the whole body manipulations reviewed above tend to have strong effects on body weight control.

Although aspects of body weight regulation are well characterized to be regulated in peripheral tissues, the master orchestrator of these players lies in the brain: the hypothalamus. The hypothalamus has been known for many years to be the central homeostatic regulator, with its outputs altering all axes of body weight regulation: food intake, thermal- and activity-based energy expenditure, and body composition. As noted above, the manipulations of ceramide metabolism that affect body weight are typically whole-body manipulations with either constitutive genetic knockouts or pharmacologic means rather than targeted to peripheral metabolic tissues such as liver, adipose tissue, and muscle. This suggests that the control of body weight by ceramide is accomplished outside of these peripheral, metabolically-important tissues. As the hypothalamus is another vital player in the control of body weight, the data reviewed above suggest the hypothesis that paradigms which modulate ceramide metabolism exert their effects on body weight through altering brain ceramide metabolism. Generally, hypothalamic lipid metabolism is becoming recognized as a participant in body weight regulation [reviewed in 42], and recent evidence suggests that sphingolipids specifically play a key role in altering hypothalamic control of body weight.

Importantly, multiple reports demonstrate that ceramide content is increased in the hypothalami of mice in obesity or in response to lipid infusions[43, 44], suggesting that hypothalamic weight control may be impaired by ceramide accumulation during the evolution of obesity. To

understand the importance of ceramides in central body weight regulation, investigators have successfully modulated hypothalamic ceramide levels by applying pharmacologic agents, hormones, or short-chain ceramides to the brain through intracerebroventricular cannulae. These studies have revealed a few interesting insights into sphingolipid influences on central control of body weight. First, hypothalamic ceramide synthesis and degradation appear to be mediated in part by hormonal cues; acute administration of leptin [45] or ghrelin [46] rapidly alters ceramide content in mouse hypothalamus. These changes in ceramide content (decreased by leptin, increased by ghrelin) are congruent with the hormones' effects on food intake (decreased by leptin, increased by ghrelin), supporting a role for dynamic alterations in ceramide content in controlling food intake. In agreement, arcuate nucleus infusions of myriocin (which blocks ceramide synthesis) were able to decrease food intake, consistent with the effects of leptin and ghrelin on both food intake and ceramide levels. Interestingly, infusion of ceramide itself does not acutely alter food intake, despite being able to block leptin-induced decreases in food intake [45-47]. This raises the question: why does altering ceramide content indirectly (by modulating synthesis or disposal via hormonal or pharmacological methods) alter food intake, but directly increasing ceramide content (with exogenous supply) does not? Many plausible explanations exist, including differences in the sites of endogenous ceramide synthesis compared with the effects of a broad ceramide delivery, an insufficient mass of C2 ceramide being provided to recapitulate an opposing effect to myriocin, or myriocin-mediated changes in the content of other sphingolipids.

Aside from its effects on food intake, one report has also demonstrated that infusion of ceramide into the hypothalamus reduces energy expenditure (without altering food intake) by reducing sympathetic outflow to brown adipose tissue[47], resulting in increased body weight. This effect was attributed to ER stress-mediated alterations in ventromedial hypothalamus (VMH) function; when chaperone protein was exogenously supplied via adenovirus, ceramide-induced ER stress in the VMH

was reversed and brown adipose tissue function was restored. Interestingly, the report also demonstrated that central ceramide administration can induce insulin resistance, which was similarly reversed by reducing ER stress. Further recent work has demonstrated that ceramide levels are dynamically altered in the hypothalamus by thyroid hormone, and that this action is important in the control of brown adipose tissue (and subsequently body weight) by the VMH[48].

Though less studied than the hypothalamus in relation to obesity, the hippocampus is also beginning to be appreciated for its role in central control of body weight[reviewed in 49]. One report has noted that AAV-Cre mediated knockout of hippocampal lipoprotein lipase (LPL) in mice causes increased hippocampal ceramide content, which drives weight gain through decreasing energy expenditure independent of changes in food intake[50]. Importantly, blocking ceramide synthesis with myriocin in the hippocampus rescues the body weight and energy expenditure phenotypes in these animals. Similarly, tyloxapol (an LPL inhibitor) injections into the hippocampus of rats had identical effects as the mouse LPL knockout, which were again reversed with myriocin treatment[50].

To our knowledge, only two reports of non-AAV-mediated genetic manipulations of sphingolipid metabolism targeted to the central nervous system exist. Using tamoxifen-inducible conditional genetics, investigators have deleted GCS in neurons of developed animals. These neuronal GCS knockout animals become remarkably obese, a finding attributed to alterations in leptin receptor signaling in hypothalamic neurons[51]. Importantly, ceramide levels in the hippocampus were noted to be unchanged in GCS knockout animals, while ceramide content in the hypothalamus was not reported. Further, this group reported in a separate study that knocking out GCS in neurons also alters hypothalamic insulin receptor signaling while blunting fasting-induced lipolysis in adipose tissue[52], again supporting a role of central glycosphingolipids in controlling whole-body metabolism.

Thus, a small but growing body of literature has begun linking regulation of ceramide content within the hypothalamus and hippocampus to neuronal output regulating insulin sensitivity, body weight, food intake, and brown adipose tissue function. A critical question remains, however: how does ceramide accumulation in the context of obesity affect neuronal function? One possibility is that ceramides affect neuronal receptor signaling with mechanisms that have been well-characterized in peripheral tissues, including the activation of the kinase PKCζ and protein phosphatase 2A and subsequent inhibition of PI3K-Akt signaling[53, 54]. In peripheral tissues, this action is vital in the context of insulin receptor inhibition by ceramide accumulation. As insulin receptor signaling plays a vital role in neuronal control of metabolism when knocked out of whole brain or discrete neuron populations[55-59], it is attractive to postulate that ceramide-induced decrements in insulin receptor signaling in the brain is one mechanism by which ceramide alters body weight control. Similarly, the adipokine leptin is known to be vital to central control of body weight[60-62]. Interestingly, leptin can also activate PI3K-Akt signaling, and these effects are also important for central control of metabolism[63]. Thus, ceramide-driven impairments in leptin-induced PI3k-Akt signaling may also be a mechanism by which ceramide influences body weight control. Alternatively, it has been demonstrated that alterations in sphingolipid content can alter neurogenesis [reviewed in 64], which may play a key role in the hypothalamic control of metabolism[65, 66]. Finally, ceramides are integral to lipid raft formation, which plays a role in synaptic plasticity[reviewed in 67]; ceramide accumulation during high fat feeding may therefore alter synaptic function in neurons which control metabolism.

Considerations and future directions

The above studies of central ceramide and body weight control, while certainly valuable, do have some important drawbacks that bear consideration. First, the pharmacologic studies uniformly apply exogenous short-chain ceramides or sphingolipid synthesis inhibitors through invasive cannulae to various regions of the brain. This does not replicate well any subtleties that may exist in physiologic

rates of ceramide synthesis, disposal, and spatial distribution, instead allowing for a broad bathing of the target region in ceramide or inhibitor. At a discrete level, it is impossible to dissect the effects of ceramide accumulation in different cell types; neuronal nuclei are highly heterogeneous, particularly those in the metabolically-important hypothalamus. Furthermore, owing to the difficulty of chronic studies where brain manipulations are concerned, the above studies were completed in acute time-courses; conversely, it is plausible that many of the effects of ceramide accumulation require both a longer time course and an endogenous accumulation/disposal pattern. Finally, injections into brain regions are not perfectly accurate; spillover into various nearby nuclei (or in the case of ventricular injections, more distant brain regions) is certainly expected.

To complement these studies, we would propose various improvements. First would be longer-duration pharmacologic interventions. For instance, mini-pumps delivering myriocin, L-cycloserine, C2 ceramide, or GCS inhibitors directly ventricles or brain regions could be utilized which last multiple weeks rather than the above paradigms which lasted at most 5 days; mini-pumps are commercially available to satisfy these specifications. This would better mimic the chronic time-course of high-fat diet induced obesity and any changes which require more than a hours or days to occur. Further, we predict that experiments altering rates of ceramide synthesis and degradation in their endogenous contexts will be more instructive than experiments dumping exogenous lipids into central structures in an indiscriminate manner.

Of greater importance, however, would be the expanded use of genetic mouse models that alter ceramide synthesis/disposal in the CNS. These models allow much greater temporal, spatial, and pathway-specific control over the manipulations of ceramide concentrations. Importantly, many of the requisite mouse lines have already been generated for study in other contexts: many neuron-specific Cre recombinase lines have been generated by neuroscientists, and a number of loxP-flanked ceramide synthesis enzymes, derivation enzymes, and sphingolipid receptors have been generated by lipid

biologists. It is vital that studies which aim to alter sphingolipid synthesis and degradation in neurons be done in an inducible manner. Aside from the standard concerns of developmental and synaptic programming of hypothalamic neurons[68], sphingolipids (and glycosphingolipids in particular) are known to be vital for neuronal development; constitutive whole-body knockouts of glucosylceramide synthase, ceramide galactosyltransferase, ceramide kinase, and acid sphingomyelinase in humans and mouse have led to severe neurological and behavioral defects, sometimes to the point of lethality[69-72]. Thus, to ensure that proper developmental programming of neurons is retained, inducible models of sphingolipid perturbation should be utilized, such as tamoxifen-inducible cre and doxycycline-inducible Tet-on/Tet-off systems should be used.

Chapter 2

High fat feeding alters sphingolipid metabolism in a tissue-specific manner

Introduction

To date, a thorough examination of sphingolipid metabolism in response to high fat feeding has not been reported in the literature. Although it is well-characterized that ceramides and other sphingolipids play a role in body weight control (see **Chapter 1**) and insulin sensitivity[7], little is known of the kinetics and tissue distribution of these effects in the evolution of obesity. Indeed, numerous reports have measured ceramide content in a tissue of interest after sundry manipulations such as inflammatory insults, high fat diet, and genetic obesity. However, none have systematically interrogated changes in the expression of enzymes of sphingolipid metabolism in response to metabolic stress. To examine this, we have completed a time-course analysis of the expression of sphingolipid metabolism enzymes in response to high fat feeding.

Methods

Animals and diets. C57Bl6 mice were bred in-house. Animals were kept on a standard 12-hr light:dark cycle. Starting at 10-weeks of age, animals were randomly assigned to groups, and provided the designated diet. Chow diet was composed of 23.9% protein, 5% fat, and 48.7% carbohydrate, while high fat diet was comprised of 20.5% protein, 36% fat, and 36% carbohydrate (Bio Serv). All animal experiments were approved and done according to the standards of the University of Texas Southwestern Medical Center Institutional Animal Care and Use Committee.

ITT-sacrifice. Animals were fasted for 3-hr before an injection of insulin (0.75 U/kg). Blood glucose was monitored for thirty minutes before animals were sacrificed. Tissues were rapidly dissected and snap frozen in liquid nitrogen.

mRNA measurement. Tissue mRNA was extracted using Trizol and converted into cDNA with a commercially-available kit according to the manufacturer's instructions. qPCR was carried out in a Roche qPCR machine using the primer sequences in Table 2.1. *Gapdh* or *Rps18* were used as housekeeping genes.

Results

High fat feeding induces hyperglycemia. To assay the effect of HFD-feeding on the enzymes of sphingolipid metabolism, we provided 10-week old animals with either chow or HFD for varying lengths of time, as demonstrated in **Fig 2.1A**. Despite 60 days of HFD feeding, there was no significant change in body weight during the experiment (**Fig 2.1B**), likely due to the effect of age-dependent susceptibility to HFD-weight gain; younger animals are relatively resistant to HFD-induced weight gain compared to more mature animals. At the end of the dietary intervention, an insulin tolerance test was performed on animals prior to sacrifice and tissue harvest. As expected, 2 months of HFD was sufficient to cause fasting hyperglycemia (**Fig 2.1C**), which was maintained throughout the course of an insulin tolerance test (**Fig 2.1D**).

Enzymes of sphingolipid synthesis are increased in skeletal muscle, but decreased in heart in response to HFD. Following the insulin tolerance test, three skeletal muscles (diaphragm, soleus, and quadriceps) were isolated along with heart, and the mRNA of sphingolipid synthesis enzymes were measured. In diaphragm (**Fig 2.2A**), soleus (**Fig 2.2B**), and quadriceps (**Fig 2.2C**) a consistent increase in the expression of ceramide synthases was noted (*Cers1-6*) with high fat feeding, while the various ceramidases (*Asah1, Asah2, Acer2,* and *Acer3*) tended to increase to a much lesser extent or not at all. Furthermore, enzymes of sphingolipid modification (*Cerk*, *Ugcg*, and *Sk2*) changed in a tissue-dependent manner; in diaphragm and soleus, little change was noted in response to HFD, while quadriceps from HFD-fed animals demonstrated an upregulation in both *Cerk* and *Sk2*. In stark contrast to the interrogated skeletal

muscles, heart responded to HFD by broadly decreasing most enzymes of ceramide synthesis (**Fig 2.2D**) while also decreasing enzymes of ceramide degradation and sphingolipid modification.

Enzymes of sphingolipid synthesis are decreased in the adipose tissue during high fat feeding. Similarly, the enzymes of sphingolipid metabolism were interrogated in subcutaneous white adipose tissue (sWAT). In SWAT, we were surprised to find striking decreases in many enzymes of sphingolipid synthesis and metabolism during the time-course of HFD-feeding, with most ceramide synthases and both *Spt1* and *Spt2* being strongly suppressed after only a day of HFD (**Fig 2.3A**). Enzymes of sphingolipid modification (*Sk1, Sk2, Ugcg, and Cerk*) were also either unchanged or decreased in response to HFD.

Enzymes of sphingolipid synthesis are decreased in liver and small intestine of HFD-fed mice. In the liver of HFD-fed mice, enzymes of sphingolipid synthesis were generally either unchanged or decreased with high fat feeding (**Fig 2.4A**). Interestingly, *Cers1-5* demonstrated a trend toward decreasing with high fat diet; in stark contrast to the other enzymes, *Cers6* was increased in the liver after two months of HFD. Similarly, in the small intestine most enzymes of sphingolipid metabolism were either unchanged or decreased, again with the notable exception of *Cers6* which was strongly increased even after just one day of HFD (**Fig 2.4B**).

Enzymes of sphingolipid synthesis are not increased in the brains of HFD-fed mice. Following the insulin tolerance test, the hypothalamus and hippocampus were dissected from rest of the brain, and the mRNA of sphingolipid synthesis enzymes was measured. Transcriptional control of sphingolipid metabolism enzymes was remarkably tight in the brain regions interrogated in response to HFD. In hypothalamus (**Fig 2.5A**), no significant changes in any enzymes of sphingolipid metabolism was noted, although a trend to decreases in some of the ceramide synthesis enzymes was observed. In the hippocampus (**Fig 2.5B**), some enzymes of ceramide synthesis were significantly decreased in HFD-fed animals, while ceramide degradation and modification enzymes were mostly unchanged. Finally, in the

remaining brain (**Fig 2.5C**) no consistent changes in response to HFD were noted, although expression of two enzymes of ceramide synthesis increased and expression of three enzymes of ceramide degradation decreased. As we were particularly surprised by the lack of any noticeable changes in the hypothalamus, we wished to validate our dissection and cDNA preparation. To do this, we also measured neuropeptides specific to the hypothalamus from these animals, and noted that (as expected from properly prepared tissues) there was a strong increase in the mRNA of *Pomc* and *Agrp* detected, two proteins enriched in the hypothalamus (**Supplementary Figure 2.1A**). Similarly, we measured *Dlg3* as a marker of the hippocampus, and noted a strong increase in *Dlg3* in the hippocampus when compared to both hypothalamus and brain (**Supplementary Figure 2.1B**).

Discussion

Despite the growing body of literature demonstrating the importance of ceramide accumulation in various metabolic tissues during obesity, this report is the first (to our knowledge) to describe the tissue-specific contributions to sphingolipid synthesis and degradation in response to high fat feeding. Importantly, this study was structured to minimize any potential body weight effects on the expression of enzymes of sphingolipid metabolism by sacrificing all animals at identical age and beginning longer-duration high fat diet feeding in younger animals. Thus, the longer-duration HFD-feeding cohorts started at younger ages (**Fig 2.1A**), when mice are less susceptible to HFD-induced weight gain. At the time of sacrifice, a trend of increased body weight was evident in animals fed HFD for longer timespans, but there were no significant differences between groups(**Fig 2.1B**), therefor avoiding any confounding changes in sphingolipid metabolism that may occur with increased body weight.

Interestingly, the only tissue where broad increases in the enzymes of ceramide synthesis were observed was in the skeletal muscles. This was particularly surprising to us, as adipose tissue and liver are known to have extremely important roles in sphingolipid metabolism; selectively reducing ceramide

content in either adipose or liver is sufficient to massively improve insulin sensitivity[35, 38]. We had previously considered muscle as a mostly passive tissue in the scheme of ceramide accumulation, acting as a pool for increased ceramide and becoming insulin resistant in response. The finding that muscle may play a comparatively outsized role in driving *de novo* synthesis of ceramide is both surprising and important; this may be key in the understanding of whole-body sphingolipid metabolism in the context of obesity. Interestingly, these effects do not extend to heart tissue and indicates a strong specificity for skeletal muscle rather than cardiac muscle in altering ceramide synthesis in response to high fat diet.

The fact that the ceramide synthases (*Cers)* do not increase in adipose tissue or liver (other than *Cers6*) during HFD may be key to our previous finding that *Asah1* overexpression is able to decrease ceramide content in these tissues and drive improvements in insulin sensitivity[38]. The product of *Asah1*-mediated degradation of ceramide (and indeed all ceramidase activity) is sphingosine, which can be converted by *Cers* back into ceramide in the classical ceramide salvage pathway[73]. Therefore, the increase in *Asah1* by genetic overexpression in our previous models will not be compensated for by increased *Cers* activity during high fat feeding in these tissues; indeed, the decreases in *Cers* in liver and adipose may render these tissues particularly susceptible to *Asah1* overexpression during HFD. Conversely, we have overexpressed *Asah1* in muscle, and seen little effect on both tissue ceramide accumulation and insulin sensitivity following HFD(unpublished observations). We can now conclude that this effect is likely due to the massive upregulation of *Cers* in muscle, which will rapidly convert the sphingosine generated by *Asah1* activity back into ceramide, rendering muscle relatively resistant to the effects of ceramidase overexpression.

We were particularly surprised by the relative lack of any changes in the expression of sphingolipid metabolism enzymes in the hypothalamus, as we and others have previously demonstrated that ceramide content is enriched in the hypothalami of high-fat fed and lipid-infused mice[43, 44], and also in context of the work described in **Chapters 3-4**. Similarly, hippocampal ceramide metabolism has

been implicated in the control of body weight, with increases in hippocampal ceramide being correlated to reduced energy expenditure[50]. Our data demonstrate a reduction in hippocampal expression of ceramide synthesis enzymes after high fat feeding, arguing against the direct induction of a ceramide synthesis program in the hippocampus being a causative factor in HFD-induced weight gain. Similarly, hypothalamic expression of sphingolipid synthesis enzymes was also unaltered, arguing against any direct effects of sphingolipid metabolism in the hypothalamus.

Although high fat diet tended to decrease or leave unchanged the expression of sphingolipid synthesis enzymes in the liver, the notable exception was *Cers6*. Interestingly, *Cers6* has been knocked out in the liver of mice previously, and demonstrated improved insulin sensitivity and decreased body weight gain. What was striking, however, was the time course of this effect, which did not occur in liver *Cers6* knockout mice until 2 months of HFD feeding had been completed; in our studies, we did not see a significant upregulation of *Cers6* in liver until 2 months of HFD were consumed. Thus, this provides evidence of the proof of principle that alterations in the expression of sphingolipid synthesis enzymes during HFD bare important consequences for whole-body metabolism.

Table 2.1

Gapdh	5’-AACTTTGGCATTGTGGAAGG	5’-ACACATTGGGGGTAGGAACA
Rps18	5’- CATGCAGAACCCACGACAGTA	5’- CCTCACGCAGCTTGTTGTCTA
Spt1	5’-TACTCAGAGACCTCCAGCTG	5’-CACCAGGGATATGCTGTCATC
Spt2	5’-ATGAAGTTGGGGATCTGCTG	5’-AGGGAGCACCAGAAAGGC
Kdsr	5’-AGAGTAGGCCGTGAAACCA	5’-TACCTGGGCAGCGTGTAC
Cers1	5’-CTGTTCTACTTGGCCTGTTG	5’-TCATGCAGGAAGAACACGAG
Cers2	5’-GTGGAGGTAGACCTTTTGTCAC	5’-CTGGCTTCTCGGAACTTTTT
Cers3	5’-TGTATAAGTGGGAAGCTTTCAC	5’-AATGTTTCAGACGTTTAGAAAATGGT
Cers4	5’-TGTCGTTCAGCTTGAGTGAG	5’-AGCAGGCTTCACAGAATTTC
Cers5	5’-CTCCAACGCTCACGAAATTC	5’-ATGCAGACAGAAGATGAGTG
Cers6	5’-GTTCGGAGCATTCAACGCTG	5’-CTGAGTCGTGAAGACAGAGG
Des1	5’-CACCGGTACCTCGGAGCGGA	5’-GTTTGGGATTGATGAACAGGGGT
Smpd1	5’-ACTCCACGGTTCTTTGGGTTC	5’-CGGCGCTATGGCACTGAAT
Smpd3	5’-ACACGACCCCCTTTCCTAATA	5’-GGCGCTTCTCATAGGTGGTG
Smpd4	5’-ATGGCGTTCCCTCACCTACA	5’-TGGCTGGAAAATCCTCAATGAC
Asah1	5’-CAGGACTGTTCAGTCTTTCAC	5’-GAGTGATAAACCCTACCCACT
Asah2	5’-GCAAAGCGAACCTTCTCCAC	5’-AGGGCCACTGTGATGACTGT
Acer2	5’-AGGGGAAGTGAAAGGAGGAG	5’-GTGTGACAATGTGCGTGTGT
Acer3	5’-CAAGTCTTTGGGGGGTTCT	5’-TCTGGCCAGCAGTCATGTT
Cerk	5’-CGGTACTGGTGTCGGAGATCA	5’-GTGAATGCGAACGGATTTTCC
Ugcg	5’-GCACATGAAGAAGACCATGATAT	5’-GAGAATTAACATGCTTCCTGCTA
Sk1	5’-CTGACGTGGACCTCGAGAGT	5’-ACAGGAAGGTAGGCCAGTTGG
Sk2	5’-CACGGCGAGTTTGGTTCCTA	5’-CTTCTGGCTTTGGGCGTAGT
Ormdl1	5’-CCCACAGTGAGGTAAACCC	5’-CAGGAACACTGCAGAAGGG
Ormdl2	5’-CTTCGCTGTGTGCCACCC	5’-GAGACAGCTGGGGAACAAG
Ormdl3	5’-GATGGCCAGCACGTAGGA	5’-CAGTCAAGAGGGGTGGCA
Nogo-A	5’-TGCTGATAAGTTACCAAGGTATCC	5’-GTTTCGTCTGGTCAAGAGGATTT
Nogo-B	5’-ACACTGACAATGCTGAACACTG	5’-AGGGGCTCGGGCTCAGT
Nogo-C	5’-GAGCAAGCTGACGCAGTACAAT	5’-AAGGTAGCTCCATTTGGCAT
Pomc	5’-CGCTCCTACTCCATGGAGCACTT	5’-TCGCCTTCCAGCTCCCTCTTG
Agrp	5’-ATGCTGACTGCAATGTTGCTG	5’-CAGACTTAGACCTGGGAACTCT

Table 2.1: qPCR primer sequences

Figure 2.1

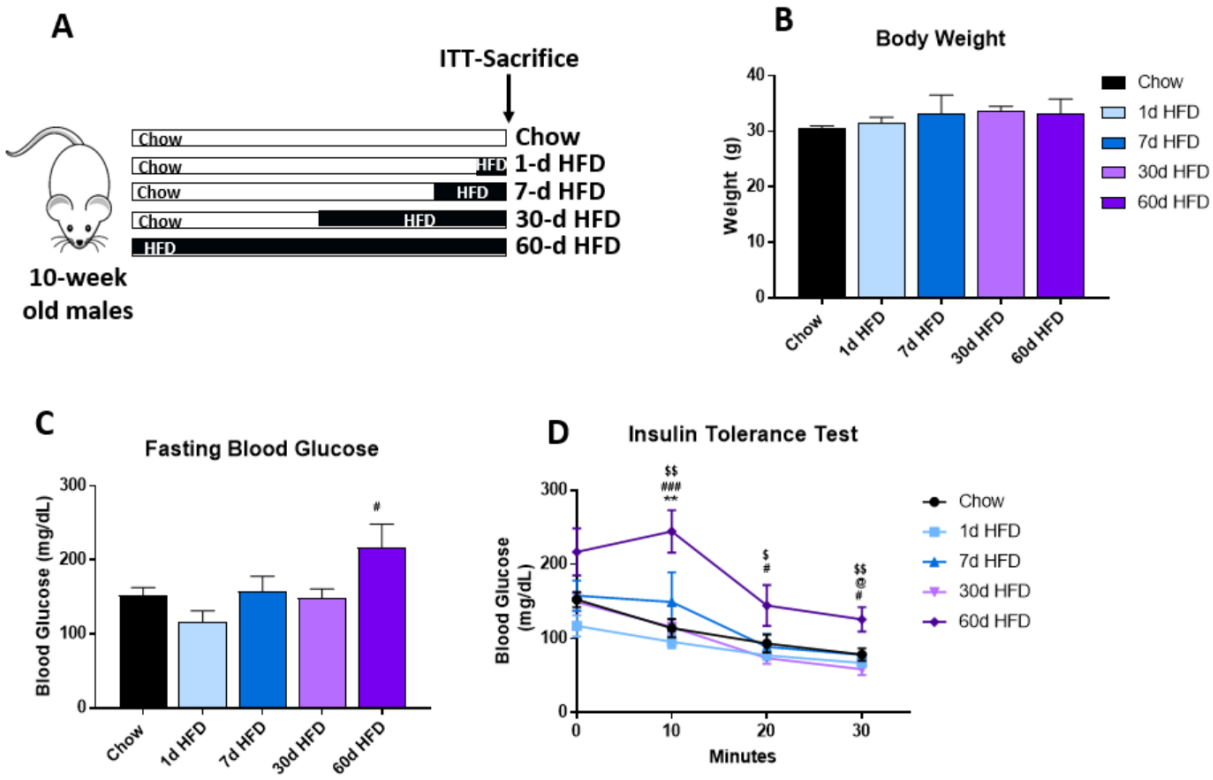

<u>Figure 2.1</u> High fat feeding causes hyperglycemia in weight- and age-matched mice. **A)** Schematic of experimental set-up. Beginning at 10 weeks of age, animals were provided chow or HFD for the indicated intervals. Prior to sacrifice, animals were fasted and an insulin tolerance test was performed. **B)** Body weights were measured at the end of the dietary intervention. **C)** Blood glucose was measured after a 3-hour fast. **D)** Insulin tolerance tests were performed at the end of the dietary intervention. Data shown as mean ± SEM. n = 4-6 per group. * $p < 0.05$ vs. chow, # $p < 0.05$ vs. 1-day HFD, @ $p < 0.05$ vs. 7-days HFD, $ $p < 0.05$ vs 30-days HFD.

Figure 2.2

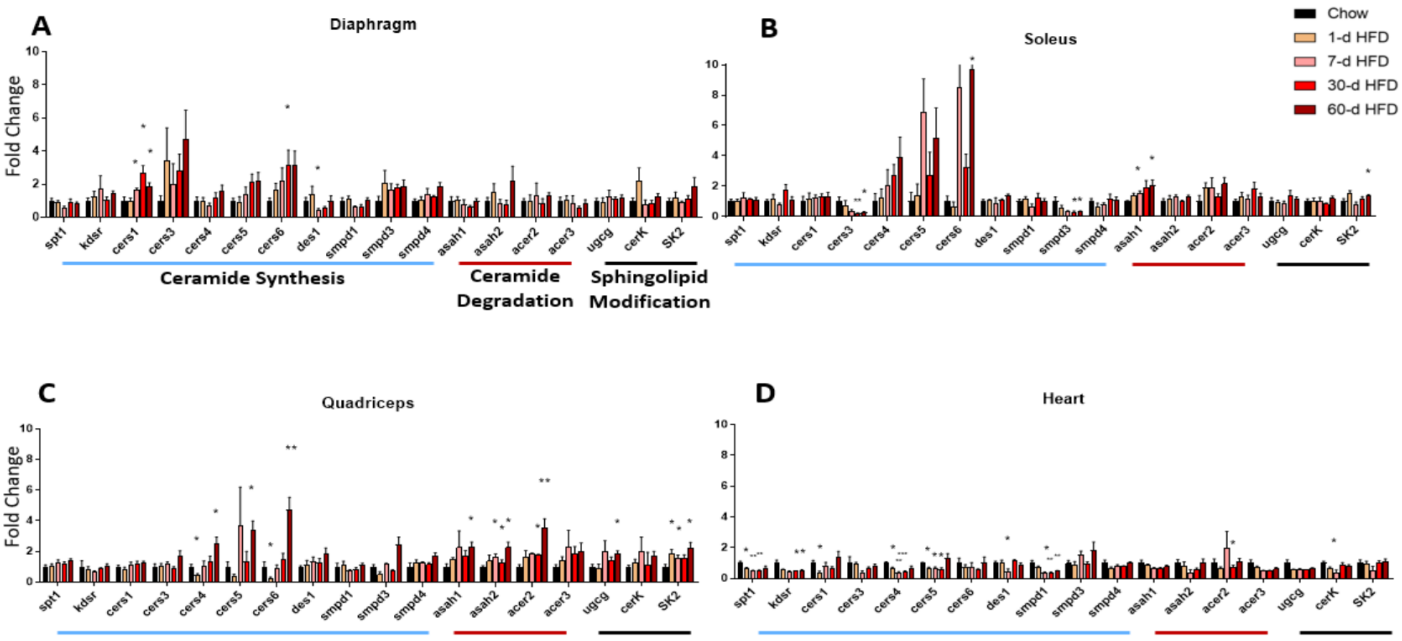

<u>Figure 2.2</u> Measurement of sphingolipid metabolism enzymes in skeletal muscle and heart during high-fat feeding. Muscles were dissected at the end of the insulin tolerance test. mRNA from the enzymes of sphingolipid metabolism was then measured in **A)** diaphragm, **B)** soleus, **C)** quadriceps, and **D)** heart. Enzymes of ceramide synthesis are denoted by a blue underscore, enzymes of ceramide degradation are denoted in a red underscore, and enzymes which modify sphingolipids (e.g. phosphorylation) are denoted by a black underscore. Data are shown as fold induction over WT as mean ± SEM. * $p < 0.05$ vs. chow. n = 4-6 per group.

Figure 2.3

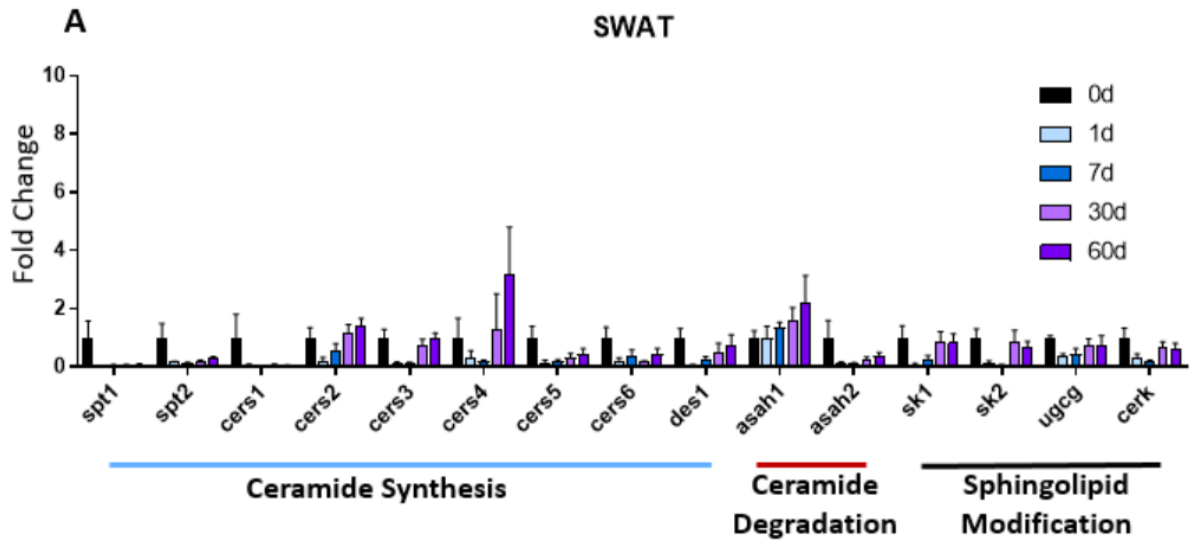

Figure 2.3 Measurement of sphingolipid metabolism enzymes in adipose during high-fat feeding. Adipose tissue depots were dissected at the end of the insulin tolerance test. mRNA from the enzymes of sphingolipid metabolism was then measured in **A)** subcutaneous adipose tissue. Enzymes of ceramide synthesis are denoted by a blue underscore, enzymes of ceramide degradation are denoted in a red underscore, and enzymes which modify sphingolipids (e.g. phosphorylation) are denoted by a black underscore. Data are shown as fold induction over WT as mean ± SEM. * $p < 0.05$ vs. chow. n = 4-6 per group.

Figure 2.4

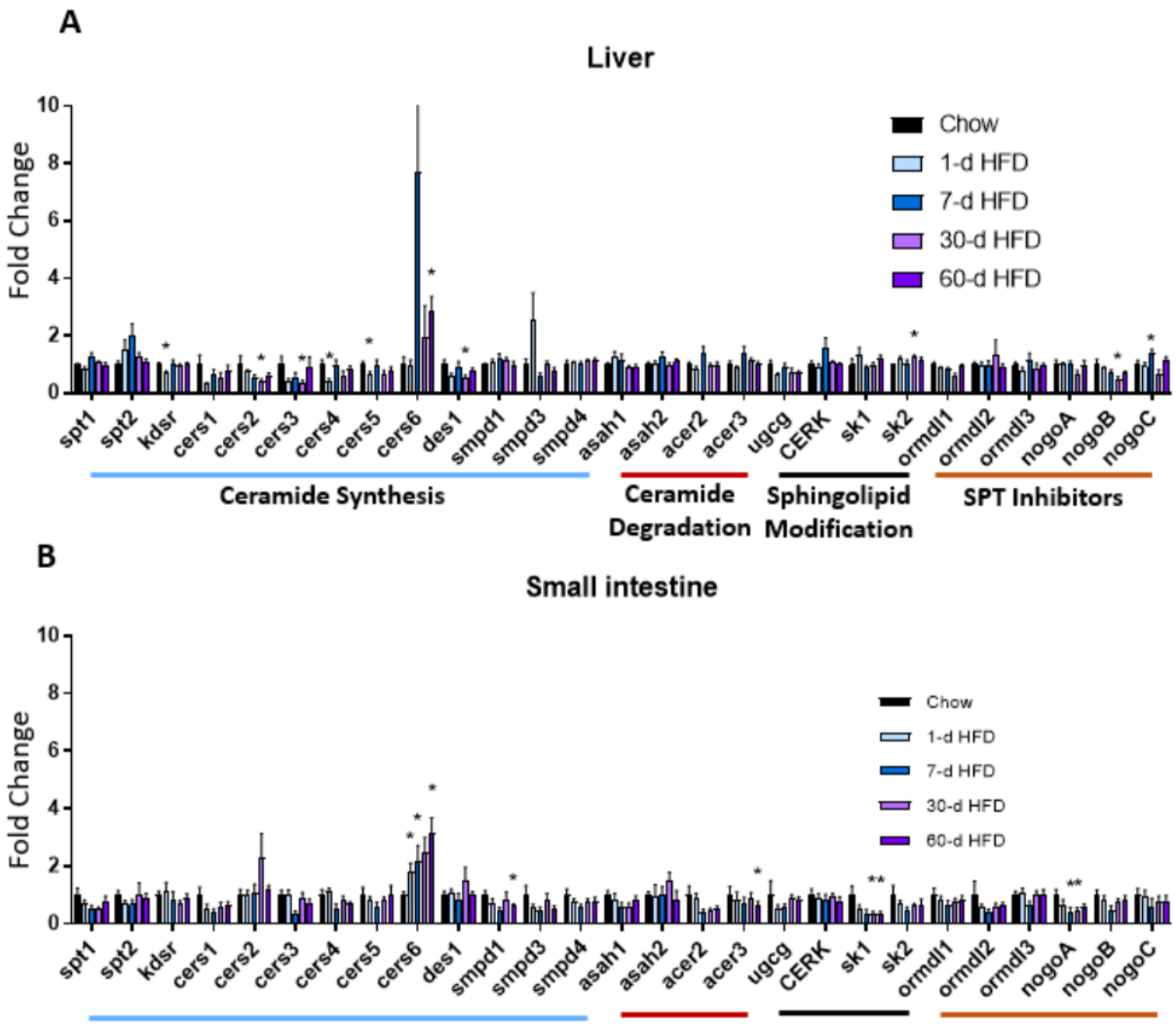

<u>Figure 2.4</u> Measurement of sphingolipid metabolism enzymes in visceral organs during high-fat feeding. Visceral organs were dissected at the end of the insulin tolerance test. mRNA from the enzymes of sphingolipid metabolism was then measured in **A)** liver and **B)** small intestine. Enzymes of ceramide synthesis are denoted by a blue underscore, enzymes of ceramide degradation are denoted in a red underscore, enzymes which modify sphingolipids (e.g. phosphorylation) are denoted by a black underscore, and enzymes which modify SPT activity are denoted by an orange underscore. Data are shown as fold induction over WT as mean ± SEM. * $p < 0.05$ vs. chow. n = 4-6 per group.

Figure 2.5

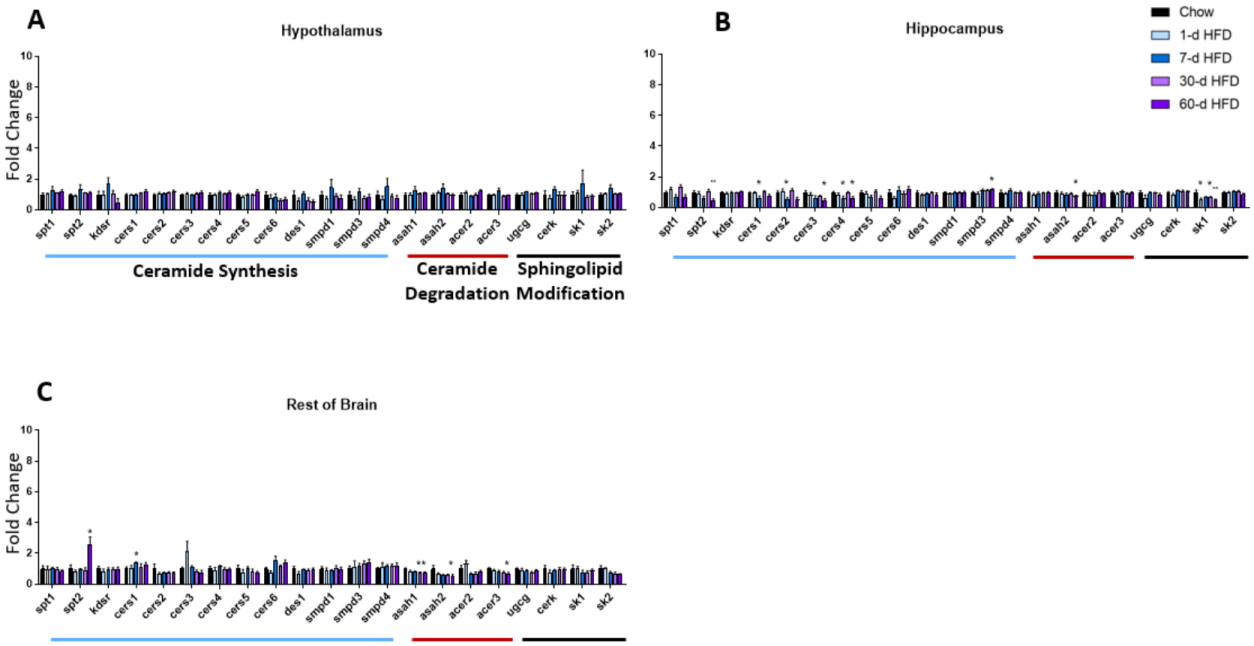

Figure 2.5 Measurement of sphingolipid metabolism enzymes in brain during high-fat feeding. Brains were dissected at the end of the insulin tolerance test. mRNA from the enzymes of sphingolipid metabolism was then measured in **A)** hypothalamus, **B)** hippocampus, and **C)** remaining brain. Data are shown as fold induction over WT as mean ± SEM. * $p < 0.05$ vs. chow. n = 4-6 per group.

Supplemental Figure 2.1

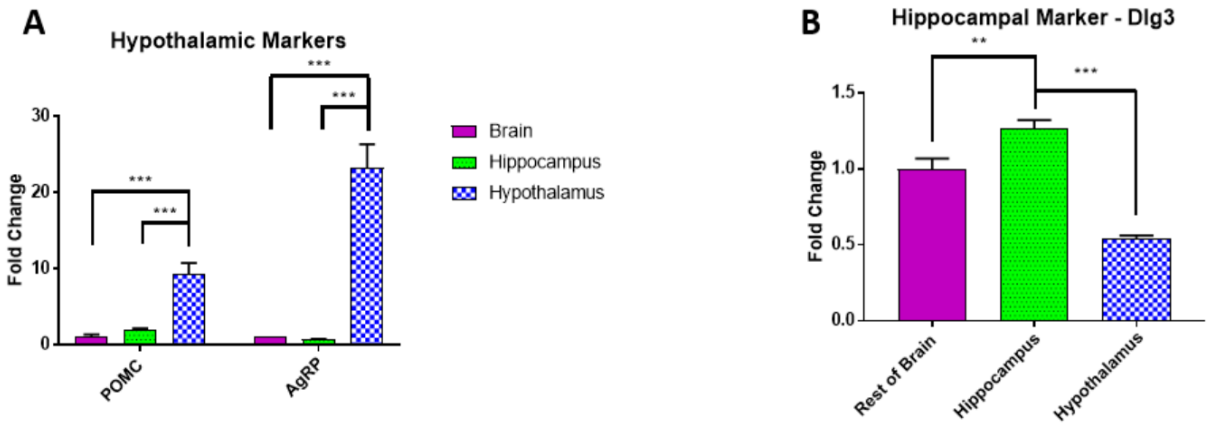

<u>Supplementary Figure 1</u> Expression of hypothalamic and hippocampal markers in dissected brain regions. A) To validate proper dissection and cDNA synthesis, two well-characterized hypothalamic markers (POMC and AgRP) were measured in brain, hippocampus, and hypothalamus from chow and 1-d HFD fed animals. **B)** To validate proper dissection of hippocampus, Dlg3 (a hippocampus marker) was measured. ** $p < 0.01$, *** $p < 0.001$. n = 7-8 per group.

Chapter 3

Ceramide accumulation in ventromedial hypothalamus during high fat feeding impairs glucose homeostasis

Introduction

Despite its broad recognition as a public health menace, obesity rates in the USA remain at record high levels[1], carrying with it an increased risk for a panoply of diseases[2]. This public health crisis points to the need for novel treatments of both obesity and obesity-related illnesses, such as cardiovascular disease and type 2 diabetes mellitus; unfortunately, success in developing anti-obesity treatments has been lacking[74]. One attractive target of recent interest has been the hypothalamus, which is vital to the control of both body weight and glucose homeostasis[75, 76]. Multiple populations of neurons reside in the hypothalamus, with diverse roles in regulating body weight control and glucose homeostasis[75, 77]. The ventromedial hypothalamus (VMH) has been recognized for its role in these actions for multiple decades[78]. Indeed, perturbations of the VMH have been shown to alter the response to hypoglycemia[79-82], muscle glucose homeostasis[83-86], and body weight regulation[55, 83, 85-87].

Sphingolipids are a broad class of lipids derived from a decarboxylation reaction of serine and palmitoyl-CoA and the addition of a second variable-length fatty acid chain[reviewed in 88]. These bioactive lipids have a role in a multitude of biological processes, and in the past few decades have become recognized to have a vital role in body weight control (reviewed in **Chapter 1**) and insulin sensitivity[reviewed in 7]. Importantly, ceramides accumulate in the hypothalamus during obesity and following intravenous saturated fat infusions [43, 44]. As hypothalamic lipid metabolism has become recognized as an important player in whole-body metabolism[42], the logical hypothesis emerges that ceramides play a role in hypothalamic control of metabolism during the evolution of obesity.

Indeed, a few recent reports point to a role for ceramides in altering hypothalamic function in its regulation of metabolism and body weight control. Two reports have indicated that altering hypothalamic ceramide content via exogenous ceramide administration or inhibitors of ceramide synthesis can change food intake[45, 46]. Furthermore, a 5-day intracerebroventricular treatment of ceramide causes reduced insulin sensitivity and increased body weight gain due to reduced brown adipose tissue energy expenditure[47]. Importantly, these effects were in part mediated by the VMH, as adenoviral delivery of chaperone proteins to the VMH could reverse the reduced brown adipose tissue energy expenditure. Finally, a recent report has demonstrated that the effects of thyroid hormone on brown adipose tissue activation are mediated in part by decreases in ceramide in the VMH[48]. As several reports are beginning to identify hypothalamic (and specifically VMH) ceramides in the control of whole body metabolism, we decided to interrogate the effect of reducing endogenous ceramides in the VMH during high fat diet-induced obesity.

Methods

Animals and diets. SF1-AC animals were generated by interbreeding of previously generated SF1-cre, rosa26-lox-stop-lox-rtTA, and tet-response-element driven AC (tre-AC)[38, 87, 89]. Animals were previously bred to a C57Bl6 background. rtTA+/tre-AC+ animals were bred to rtTA+/tre-AC+/SF1-cre+ animals to generate experimental cohorts; wild-type (WT) animals lacked SF1-cre. For electrophysiology and histology experiments, previously engineered animals carrying an engineered SF1-eGFP allele were bred to SF1-AC animals, and cre-positive animals were compared to cre-negative[90]. All animals used in these studies were littermate/cage-mate males, and all metabolic phenotyping was done on animals of identical body weight. For the high fat diet (HFD) studies, high fat-high sucrose diet containing 600 mg/kg doxycycline was utilized. The chow diet also contained 600 mg/kg doxycycline. For the pre-fattening, doxycycline-reversal experiments (**Figure 3.4E-F**), animals were provided high fat diet without dox for 6 weeks before being provided HFD-dox. All animals were kept on a standard 12-hr light:dark

cycle, and all manipulations were done between 0700-1700. Body composition was measured at the indicated time point by NMR (Bruker, Millerica, MA, USA).

Oral glucose tolerance tests. For oral glucose tolerance tests (OGTT), animals were placed in a procedure room to acclimate and fasted for 5 hours. Glucose (2.5 g/kg) was injected to the stomach via oral gavage at the end of the fast, and blood glucose was measured at the indicated points. To measure glucose-stimulated insulin secretion (**Figure 3.4C**), serum was drawn before and 15 minutes after the glucose bolus.

Insulin tolerance tests. Unless otherwise noted, animals were placed in a procedure room to acclimate and fasted for 3 hours. Insulin was prepared in PBS with a few mg of BSA as a carrier, and injected at 0.75 U/kg intraperitoneally and blood glucose was measured at the indicated points. To experimentally induce hypoglycemia for **Figure 3.5G**, animals were fasted overnight (20 hours) before being injected with a double dose (1.5 U/kg) of insulin, and serum was drawn immediately before the injection and 60 minutes after the injection to monitor glucagon secretion.

Serum insulin and glucagon measurement. For all serum insulin measurements, a commercially available insulin ELISA (Crystal Chem, Elk Grove Village, IL, USA) was used according to manufacturer instructions. For serum glucagon measurements, a commercially available glucagon ELISA (Mercodia, Uppsala, Sweden) was used according to manufacturer instructions.

Serum glucose/FFA/glycerol measurement. Serum glucose was measured with handheld glucometers (Bayer). Serum free fatty acids and glycerol were measured with reagents according to manufacturer instructions (Infinity, Thermo Fisher).

Serum corticosterone and testosterone measurement. Serum corticosterone and testosterone were measured by the University of Virginia Ligand Assay & Analysis Core.

Gene expression. Tissues were harvested, dissected as needed, and snap frozen in liquid nitrogen. To extract mRNA, tissues were homogenized in Trizol and extracted according to manufacturer specifications (Thermo Fisher, Waltham, MA, USA). mRNA concentration was measured with a spectrophotometer, and cDNA was created using a kit according to manufacturer instructions (Thermo Fisher). Gene expression was assayed using the primers described in **Chapter 2**.

Electrophysiolgy. Electrophysiological recordings of neurons were carried out as previously described[91].

Hyperinsulinemic-euglycemic clamps. Hyperinsulinemic-euglycemic clamps were done as previously described. Briefly, animals were fasted for five hours in the morning. Next, ^{3}H-labeled glucose was infused for 90 minutes to assay basal hepatic glucose output. During the clamp, animals were clamped at 4U/kg/min insulin, and glucose infusion rate was varied until animals achieved a steady-state blood concentration of 150 mg/dL glucose.

Glucagon tolerance tests. To assay glucagon tolerance, animals were fasted for 1 hour to empty the stomach before being injected with glucagon at the indicated dose. Blood glucose was monitored at the indicated time points. To understand the effect of insulin sensitivity on the glucagon tolerance assay, myriocin (Sigma-Aldrich, 0.3 mg/kg) was injected for 3.5 weeks on an every other day schedule.

Arginine tolerance test. To assay the blood glucose response to endogenous glucagon and insulin secretion, arginine (2 g/kg) was injected into 2-hr fasted animals. Blood glucose was measured at the indicated time points, and serum was drawn at t = 0 and t = 10 minutes.

Triolein lipid test. The lipid uptake and oxidation test was performed as previously described[92]. Briefly, ^{3}H labeled triolein was incorporated into intralipid micelles and diluted in PBS before intravenous injection. After a 15-minute incubation, animals were sacrificed, and indicated tissues were harvested. Tissues were extracted in chloroform:methanol and aqueous and lipid phases were separated before

being counted in a scintillation counter. Tissue lipid oxidation and uptake is presented on a percent/g basis, normalized to WT controls.

Western blot. For immunoblotting analysis, total protein extracts were prepared from liver tissues of mice and transferred to a nitrocellulose membrane (Bio-Rad Laboratories). The blotted membrane was blocked in 1× Tris-buffered saline (TBS) containing 0.1% Tween and 5% (wt/vol) nonfat dry milk (TBST-MLK) for 1 h at room temperature with gentle, constant agitation. After incubation with primary antibodies anti–phospho-CREB, anti-CREB, anti-PEPCK (Cell Signaling Technologies), anti-glucagon receptor (Alomone Labs catalog number AGR-021), or anti–γ-tubulin (Sigma) in freshly prepared TBST-MLK at 4 °C overnight with agitation, the membrane was washed two times with TBST buffer. This was followed by incubating with secondary anti-rabbit or anti-mouse horseradish peroxidase-conjugated Ig antibodies in TBST-MLK for 1 h at room temperature with agitation. The membrane was then washed three times with TBST buffer, and the proteins of interest on immunoblots were detected by an ECL plus Western blotting detection system (GE Healthcare Life Sciences). The corresponding bands were quantified using NIH Image software (version 1.6; available at https://imagej.nih.gov/ij/).

β-*3AR stim test.* To assay adipocyte β adrenergic receptor sensitivity, random-fed animals were injected intraperitoneally with CL316,243 (Sigma-Aldrich, 1.5mg/kg) and bled at the indicated time points to measure serum blood glucose, free fatty acids, and glycerol.

Results

Generation and validation of mice overexpressing acid ceramidase in SF1-neurons. To study the effects of ceramide accumulation in the VMH during obesity in the context of metabolism, we used previously generated animals to overexpress acid ceramidase (AC) in SF1 neurons of the VMH. These animals (termed SF1-AC) are able to inducibly deplete ceramides in SF1 neurons when provided doxycycline in

the diet. To generate SF1-AC mice, previously generated and validated SF1-cre mice were bred to rosa26-loxP-stop-loxP-rtTA and tet-ON-AC mice [38, 87, 89]. Cre-mediated excision of a stop cassette allows for expression of rtTA in SF1-expressing cells. When animals are provided doxycycline in the diet, the triple transgenic SF1-AC animals will overexpress AC in cells expressing SF1, and deplete ceramide content within these cells (**Figure 3.1A**). Animals were generally obtained in the expected Mendellian ratio (data not shown). To validate overexpression of AC in SF1-expressing tissues, WT and SF1-AC animals were provided doxycycline (600 mg/kg) in high fat diet (HFD). As expected, in tissues which are known to express SF1-cre (VMH, adrenal, and testes), an increase in AC mRNA was detected in SF1-AC animals, in a dox-dependent manner(**Figure 3.1B-D**). Tissues without expression of SF1-cre did not demonstrate increased AC expression (**Supplemental Figure 3.1A**). As adrenals and testes can alter systemic metabolism through their canonical roles in the secretion of corticosterone and testosterone, we measured these hormones to ensure that changes in corticosterone and testosterone were not the reason for any ensuing phenotypic changes. Importantly, serum corticosterone (in chow and HFD-fed animals) and testosterone (in HFD-fed animals) levels were unchanged in SF1-AC animals (**Supplemental Figure 3.1B-D**), and adrenal tissue histology was grossly normal in chow-fed SF1-AC animals (**Supplemental Figure 3.1E**), arguing against any non-neuronal effects in mediating the phenotypes noted below.

Effect of increased ceramidase activity on SF1-neuron electrophysiological function. To understand the effect of acid ceramidase overexpression on neuronal integrity and function, we bred SF1-AC mice to a fluorescent SF1-eGFP reporter mouse, allowing for visualization and electrophysiological measurement of SF1-neurons in SF1-AC animals. WT::SF1-GFP and SF1-AC::SF1-GFP animals were provided high fat diet containing doxycycline for 6 weeks. GFP-labeled neurons in the VMH appeared grossly normal in SF1-AC mice (**Supplemental Figure 3.2**). Although not significant, a trend of depolarized resting membrane potential (RMP) was noted in SF1-AC animals, possibly indicating reduced threshold to

excitability (**Figure 3.2A**). However, this increase in resting membrane potential did not alter spontaneous action potential frequency (**Figure 3.2B**). Importantly, SF1-AC mice display a significant increase in the frequency of excitatory post synaptic currents (EPSC) and a trend toward an increased frequency of inhibitory post synaptic currents (IPSC) (**Figure 3.2C-D**). Similarly, a trend toward increased input resistance, and therefor increased excitability of SF1 neurons was noted in SF1-AC mice (**Figure 3.2H**). However, the evoked response to EPSCs and IPSCs remained unchanged between groups (**Figure 3.2E-F**).

VMH ceramide accumulation does not affect body weight or composition control on chow or high fat diet. As others have previously implicated hypothalamic ceramide accumulation (and specifically VMH ceramide accumulation) in altering body weight control through food intake and brown adipose tissue function, we studied the effects of VMH ceramide depletion on body weight gain and body composition. To do this, animals were provided dox-chow (**Figure 3.3A-B**) or dox-HFD (**Figure 3.3C-D**). Body weight (**Figure 3.3A & 3.3C**) was measured at the indicated time points and was unchanged through the entire experiment, while body composition (**Figure 3.3B & 3.3D**) was also unchanged when measured at three months (chow) or two months (HFD) of the experiment, demonstrating that depletion of VMH ceramides does not alter body weight or composition in SF1-AC mice in response to either chow or HFD. To assay whether tissue size was altered, tissue mass was measured for a cohort of 4-month HFD-fed animals, demonstrating no changes in the weight of any of the harvested tissues (**Figure 3.3E**).

Depletion of VMH ceramides improves glucose homeostasis. As SF1-neurons are known to regulate insulin sensitivity, we hypothesized that altering ceramide content in the VMH may alter glucose homeostasis and insulin sensitivity. To test this, we analyzed WT and SF1-AC mice fed dox-chow for 3 months. Random-fed blood glucose and insulin (**Supplemental Figure 3.3A-B**) were unchanged. Similarly, oral glucose tolerance (**Supplemental Figure 3.3C**) and insulin tolerance (**Supplemental Figure 3.3D**) were unchanged, demonstrating that VMH ceramide depletion does not alter glucose homeostasis

in chow fed animals. As it has been noted that manipulations of SF1-neurons typically require a metabolic challenge to unveil any phenotypic changes, we also assayed measures of glucose metabolism in WT and SF1-AC mice fed dox-HFD. On HFD, oral glucose tolerance was improved in SF1-AC mice without changes in insulin secretion (**Figure 3.4A-C**). Interestingly, AC overexpression in the VMH was able to strikingly improve high fat-mediated glucose intolerance in animals pre-fattened with 8 weeks of HFD before the addition of dox to the diet (**Figure 3.4E-F**). However, despite these improvements in glucose homeostasis, insulin tolerance was unchanged (**Figure 3.4D**).

To understand the mechanism driving this improvement in glucose homeostasis, we performed hyperinsulinemic-euglycemic clamps on WT and SF1-AC animals fed HFD-dox. During the clamp, there was no difference in the glucose infusion rate required to clamp the animals at steady state, and the radiolabeled-glucose disposal remained unchanged between groups (**Figure 3.4G-H**), validating the lack of change in insulin tolerance noted above. We were surprised to find, however, that hepatic glucose output was decreased in SF1-AC animals only in the basal (unstimulated) state (**Figure 3.4I**). Typically when changes in hepatic glucose output are discovered during a hyperinsulinemic-euglycemic clamp, they are found either during both the basal and clamp state, or only during the insulin-stimulated clamp state; we are unaware of any other report of a mouse model where hepatic glucose output is lower during the basal state, and not the clamp state. During both the basal and clamped state, no significant differences were detected in plasma glucose, insulin, or FFAs (**Table 3.1**).

Depletion of VMH ceramides alters glucagon sensitivity. As SF1-neurons have been well-characterized to control insulin sensitivity, we were surprised to see an improvement in glucose homeostasis but no change in insulin sensitivity in SF1-AC mice. We were particularly confounded by the insights revealed in the clamp studies, where hepatic glucose output was lowered only in the basal state. However, previous reports have demonstrated alterations in hepatic glucose output in manipulations of SF1-neurons. In VMH-lesioned rats and mice with blunted SF1-neuron signaling capability, animals are unable to defend

against hypoglycemia due to a defect in secretion of the counterregulatory hormones glucagon, epinephrine, and norephinephrine, which serve to raise blood glucose[80, 81]. As the basal (unstimulated) state of the clamp is a fasted state, we hypothesized that glucagon secretion or sensitivity was impaired in SF1-AC animals, leading to decreased hepatic glucose output and accounting for the improvements in glucose tolerance that we had noted earlier. In support of this, we noted lowered blood glucose and increased serum triglyceride in HFD-fed, overnight fasted SF1-AC mice (**Figure 3.4J-K**). The decrease in blood glucose was not a result of impaired glucagon secretion, as circulating glucagon in SF1-AC mice was not altered in either the fed or fasted condition (**Figure 3.4L**).This phenotype is reminiscent of that seen in glucagon receptor knockout animals, which have lowered blood glucose and increased fasting triglycerides[93].

We thus developed three paradigms by which to evaluate *in vivo* glucagon secretion and sensitivity. First, we used a previously validated pharmacologic intraperitoneal glucagon injection, and analyzed blood glucose through the duration of the study. In chow-fed, 5-day-HFD-fed, and 4-month HFD-fed SF1-AC animals, glucose excursion in response to glucagon was reduced (**Figure 3.5A-F**). As a comparison, we also carried out these experiments in a well-validated model of improved insulin sensitivity: HFD-fed myriocin-injected animals (**Supplemental Figure 3.4**), where reductions in blood glucose are only apparent *after* the time of glucose excursion in response to glucagon (the first ~ 30 minutes of the injection). Thus, these acute glucagon injections suggest that AC overexpression in VMH can blunt glucagon sensitivity.

Although these experiments were intriguing, they are also a response to an exogenous, nonphysiologic bolus of glucagon. Is endogenous glucagon action similarly blunted? To answer this, we fasted HFD-fed WT and SF1-AC animals for 20 hours, and then performed an insulin tolerance test at double our standard dosage (1.5 U/kg). This experimental setup will rapidly drive animals into hypoglycemia, where both endogenous glucagon secretion and action can be assessed. Although HFD-

fed SF1-AC animals were able to defend from hypoglycemia during fasting and had similar fasting glucagon levels, euglycemia was not sufficiently maintained during the insulin challenge; in response to a strong insulin bolus, hypoglycemia was reached more rapidly in SF1-AC animals (**Figure 3.5G**). Importantly, glucagon secretion in the hypoglycemic state was unchanged (**Figure 3.5H**), suggesting that the difference noted in blood glucose was due to changes in glucagon sensitivity rather than changes in glucagon secretion.

To see whether these effects could be magnified, we used a stronger stimulant of glucagon secretion: an intraperitoneal arginine injection. Arginine is well-known for its ability to depolarize pancreatic alpha and beta cells, causing massive degranulation and release of insulin and glucagon. As we have thoroughly demonstrated above, insulin sensitivity is unchanged in SF1-AC animals, so any alterations in blood glucose during the experiment must result from changes in glucagon secretion or glucagon sensitivity. Indeed, SF1-AC animals had strikingly lower blood glucose following an arginine injection, while both insulin and glucagon secretion were unchanged (**Figure 3.5I-L**). This again suggests that glucagon sensitivity is markedly reduced, as the lower blood glucose levels during the assay must result from changes in glucagon (and not insulin) sensitivity. Again, glucagon or insulin secretion was identical between groups after the arginine injection, ruling out a possibility of a defect or improvement of pancreatic hormone secretion. These experiments demonstrate that SF1-AC animals have reduced glucagon sensitivity independent of any changes in glucagon secretion.

Altered glucagon sensitivity does not arise from altered hepatic lipid uptake and oxidation or glucagon receptor signaling. To explain the alterations seen in glucagon sensitivity, we first hypothesized that changes in hepatic glucagon receptor protein or signaling had occurred. However, glucagon receptor protein levels were unaltered in the liver of SF1-AC animals, and SF1-AC mice had a surprising increase in PEPCK, the transcription of which is driven by glucagon receptor signaling (**Figure 3.6A**). Activated glucagon receptor is known to increase intracellular cAMP, which then activates protein kinase A to

phosphorylate cAMP response element-binding protein (CREB), leading to its downstream effects on glucose output and gluconeogenesis. We hypothesized that the changes in glucagon sensitivity in SF1-AC mice may be due to changes in glucagon-stimulated phospho-CREB. However, glucagon-stimulated p-CREB was also unaltered in the liver of SF1-AC mice (**Figure 3.6A**). Thus, glucagon receptor signaling is intact, and expression of both the receptor itself and its downstream effectors is unchanged, leading us to conclude that hepatic glucagon receptor signaling is grossly intact and does not cause the reduced glucagon sensitivity phenotype. We then hypothesized that hepatic energy supply was disturbed in SF1-AC mice, as this may impair the energy supply needed to drive gluconeogenesis in the liver. We thus carried out ^{3}H-labeled triolein lipid tracing experiments, where radiolabeled lipid is packaged into intralipid micelles and injected intravenously into fasted animals. This allows for measurement of both tissue lipid uptake and oxidation. In liver (and all other measured tissues), no changes in either tissue lipid uptake or oxidation were found (**Figure 3.6B-C**). To further assay adipose tissue function, we conducted β3-adrengergic receptor (β3-AR) stimulation, but did not note any changes in serum free fatty acids, glycerol, glucose or insulin, suggesting that there are no changes in β3-AR sensitivity (**Supplemental Figure 3.5**). Thus, it is unlikely that altered lipolysis, lipid uptake, or lipid oxidation impairs hepatic gluconeogenesis in SF1-AC mice.

Discussion

The above experiments represent the first demonstration of altering endogenous ceramide metabolism within targeted neuronal populations. Overexpression of acid ceramidase did not grossly impact neuronal function, as confirmed by both the electrophysiology data and the normal body weight regulation in SF1-AC mice; disruption of VMH neurons is a classical obesogenic stimulus, and thus the unchanged body weight in SF1-AC mice suggests intact VMH function[94]. The ceramidase overexpression did not change rates of spontaneous firing or evoked responses in SF1 neurons, but did increase excitability in recorded SF1 neurons from SF1-AC animals. We speculate that these effects may

be mediated by 1st order SF1 neurons synapsing onto our recorded SF1 neurons in the case of EPSCs, or in the case of IPSCs by SF1 neurons increasing activity of inhibitory neurons which then synapse onto recorded SF1 neurons. This model implies that ceramidase overexpression serves to increase spontaneous synaptic vesicle release, a hypothesis which requires further study. Separately, it has been demonstrated that ceramides play a role in lipid raft function and synaptic plasticity; altering ceramide content may alter synapse numbers, which may explain the effects seen in increasing both EPSCs and IPSCs[67].

We demonstrate here that ceramide accumulation in SF1 neurons of the hypothalamus during high fat feeding worsens glucose tolerance in a reversible manner. Further, these changes in glucose tolerance are not related to insulin sensitivity, but rather reflect changes in glucagon sensitivity through an as-yet undescribed mechanism. During the analysis of these experiments, we were continuously surprised about the differences in our findings compared to what others have reported when C6-ceramide is exogenously supplied to the hypothalamus[47, 48]; we had expected our results to be directly opposite in nature to the C6-ceramide challenges. As these reports showed that C6-ceramide blunts sympathetic nerve activation of brown adipose tissue and subsequently can increase body weight in rats, we had expected an opposite finding when overexpressing AC in the VMH of mice. However, our data clearly and consistently show over multiple cohorts of animals that there is no effect of AC overexpression in SF1 neurons on body weight regulation in both chow and high fat fed animals. Similarly, investigators noted that C6-ceramide application to the hypothalamus blunts insulin sensitivity, whereas we found no effect of acid ceramidase overexpression on insulin sensitivity during insulin tolerance tests and hyperinsulinemic-euglycemic clamps, again over multiple cohorts of animals. Although there was no effect of VMH ceramide depletion on body weight or insulin sensitivity in our studies, there was a non-significant trend toward smaller brown adipose tissue fat pads, and a similar trend toward increased lipid uptake and oxidation in those fat pads (**Figure 3.3E & 3.6B-C)**. Thus,

although our data would rule out any effect of ceramide accumulation during diet-induced obesity in SF1 neurons on body weight or insulin sensitivity, these data may agree with the effects of modulating VMH ceramides on BAT function that others have noted. Regardless, this work reveals a heretofore unknown biology of SF1 neurons in the VMH: the regulation of systemic glucagon sensitivity. It will be of interest to validate or disprove these findings in other models of SF1 neuron manipulation where changes in glucose tolerance are seen without changes in body weight.

Importantly, the lack of any noticeable phenotype in chow-fed animals argues against any effect of AC overexpression on normal neuron function; unlike some other models of perturbed SF1 neurons, chow-fed SF1-AC animals had normal body weight, body composition, and insulin sensitivity. The vast majority of phenotypic changes were only noted with high fat feeding, in agreeance with previous findings that SF1 neurons generally require a metabolic challenge (fasting, exercise, or diet-induced obesity) before seeing the effects of SF1 neuron manipulation.

Although others have demonstrated that altering hypothalamic ceramide metabolism alters insulin sensitivity, weight gain, and brown adipose tissue activation, we see none of these effects. Why are these results so divergent from other studies of ceramide in the hypothalamus? First, this work only modulates ceramide content in SF-1 neurons of the hypothalamus, whereas others have changed ceramide content or synthesis in the entire hypothalamus, where many other neuronal populations vital to the regulation of body weight and insulin sensitivity also reside. Further, these manipulations are acute, exogenous treatments rather than alterations of endogenous sphingolipids during chronic high fat feeding. Similarly, others have modulated ER stress in response to ceramide in the VMH with adenoviral-mediated gene expression; the VMH is comprised of neurons other than just SF1-neurons, and it is thus possible that those neurons mediate ceramide's effects on insulin sensitivity and body weight control. Finally, the exogenous administration of ceramide will also affect glial populations, which are rapidly being recognized as key players in the central control of metabolism[95].

Although it is known that ceramides accumulate in the hypothalamus during high fat feeding, an open question is the origin of these hypothalamic ceramides. A few possibilities exist: first, hypothalamic ceramides may be synthesized from *de novo* precursors within neurons. Second, ceramides may be delivered to and across the blood brain barrier either on lipoproteins in circulation or as constituents of freely floating lipid rafts. Finally, hypothalamic astrocytes may produce ceramide and traffic this ceramide on lipoprotein to neurons. We prefer the theory of astrocyte, as our preliminary data demonstrates a role for astrocyte sphingolipid metabolism in obesity (**Chapter 4**).

Finally, this work provides further evidence of the importance of hypothalamic ceramide accumulation in driving aspects of metabolic syndrome. It will be of interest to continue this work in other neuronal populations, and separately to focus on multiple aspects of ceramide metabolism not covered here such as alterations in endogenous synthesis and disposal pathways and perturbations of ceramide derivation (*i.e.* the production of glucosylceramide, sphingosine-1-phosphate, *etc.*).

Table 3.1

	Body Weight (g)	Basal			Clamp		
		Plasma Glucose (mg/dL)	Plasma Insulin (ng/mL)	Plasma NEFA (mmol/L)	Plasma Glucose (mg/dL)	Plasma Insulin (ng/mL)	Plasma NEFA (mmol/L)
WT	35.5±1.6	121.3±3.7	0.87±.12	0.21±.02	154.7±4.9	3.24±.23	.17±.02
SF1-AC	39.2±2.4	116.6±7.7	1.35±.23	0.22±0.01	152.6±2.8	3.3±.26	.16±.02
	p = NS for all WT vs. SF1-AC comparisons						

Table 3.1: Serum chemistry during hyperinsulinemic-euglycemic clamp.

Figure 3.1

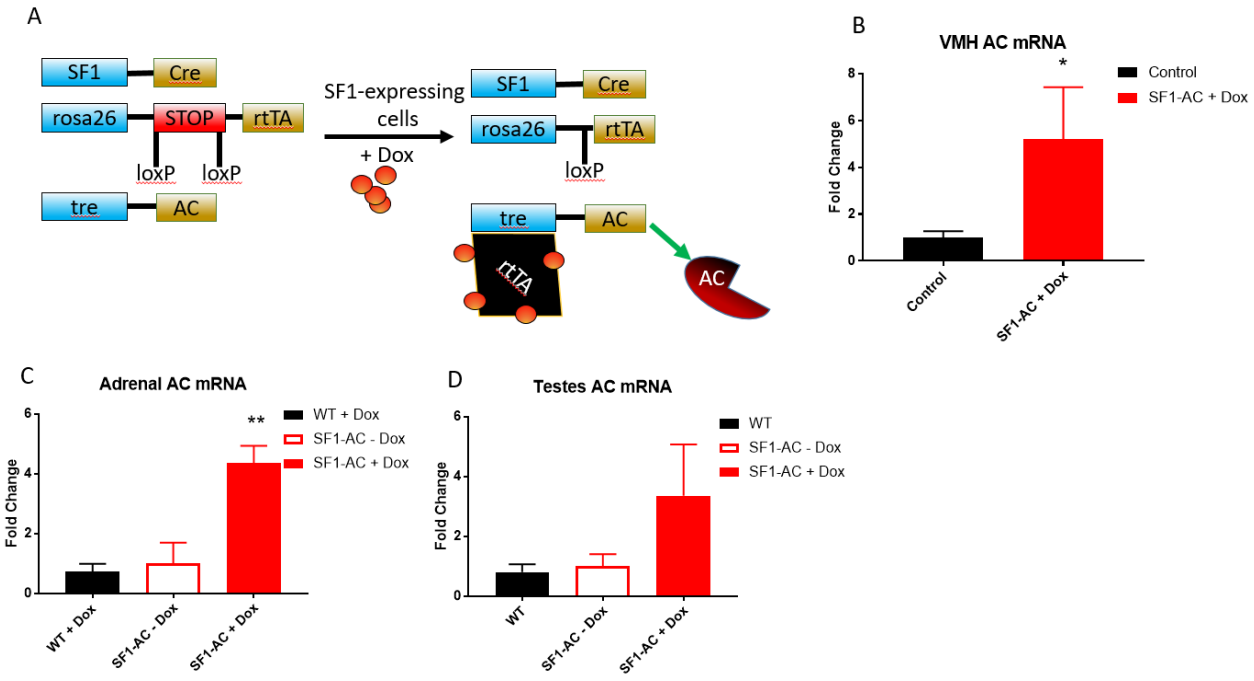

<u>Figure 3.1</u>: Validation of acid ceramidase overexpression in SF1-expressing cells. (A) Schematic of mouse genetics allowing for inducible overexpression of AC in SF1 neurons. Animals expressing Cre recombinase in SF1-expressing cells were bred to animals expressing rtTA under the control of loxP-flanked stop cassettes and tet response element-driven acid ceramidase. When animals are provided doxycycline in the diet, acid ceramidase in overexpressed in SF1-expressing tissues. Expression of acid ceramidase in SF1-expressing tissues: **(B)** VMH, **(C)** adrenal, **(D)** testes.

Figure 3.2

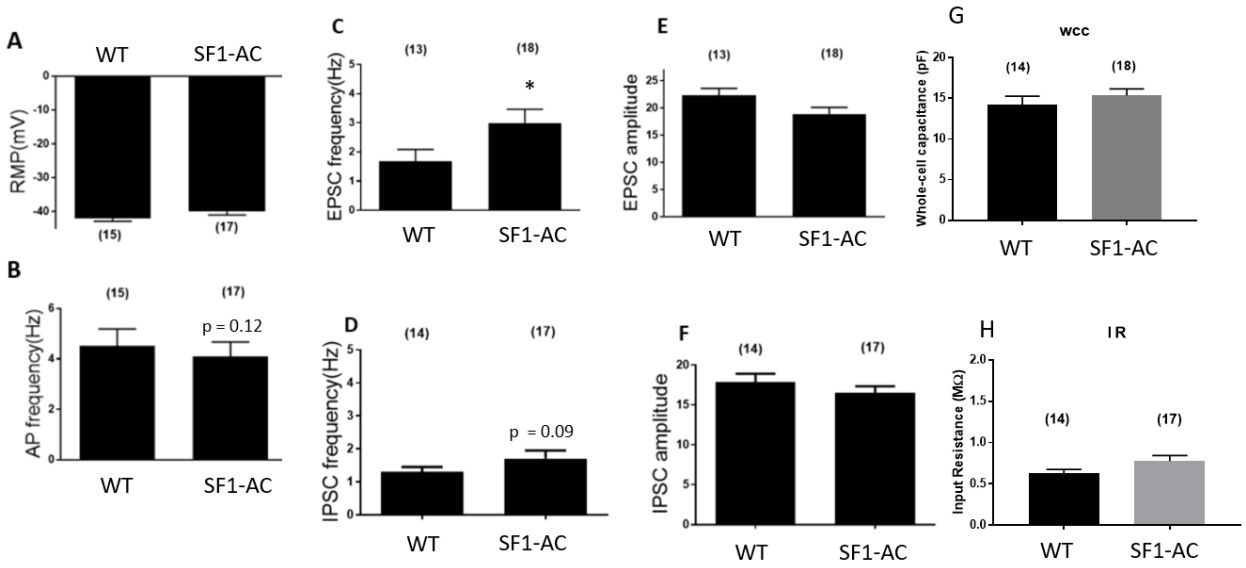

Figure 3.2: Acid ceramidase overexpression alters excitability of SF1 neurons WT and SF1-AC mice expressing an SF1-eGFP reporter fluorescent were fed high fat diet + dox for 6 weeks before electrophysiology recordings. **(A)** Resting membrane potential of SF1-GFP neurons in WT and SF1-AC mice. **(B)** Frequency of spontaneous action potentials in SF1-GFP neurons. Spontaneous excitatory post-synaptic current frequency **(C)** and amplitude **(E)** and inhibitory post-synaptic current frequency **(D)** and amplitude **(F)**.

Figure 3.3

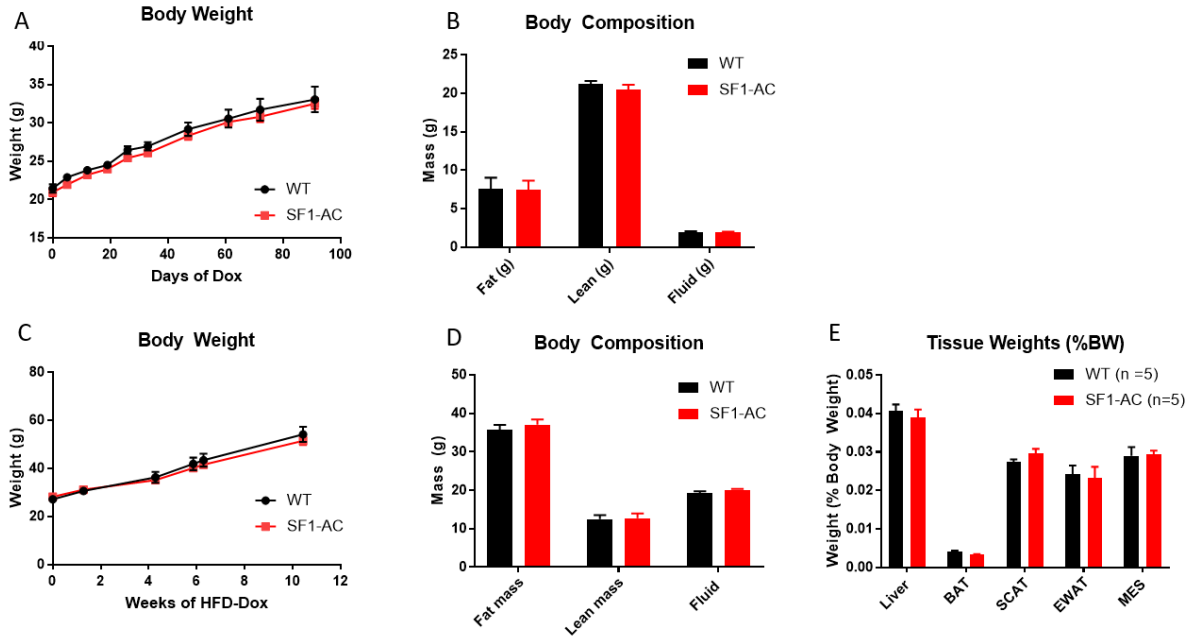

<u>Figure 3.3</u>: SF1-AC mice do not have altered weight gain or body composition on chow or HFD. WT and SF1-AC were provided chow **(A-B)** or HFD **(C-D)** containing dox. Body weights **(A&C)** were measured at indicated time points. Body composition (**B&D)** was measured by NMR prior to sacrifice.

Figure 3.4

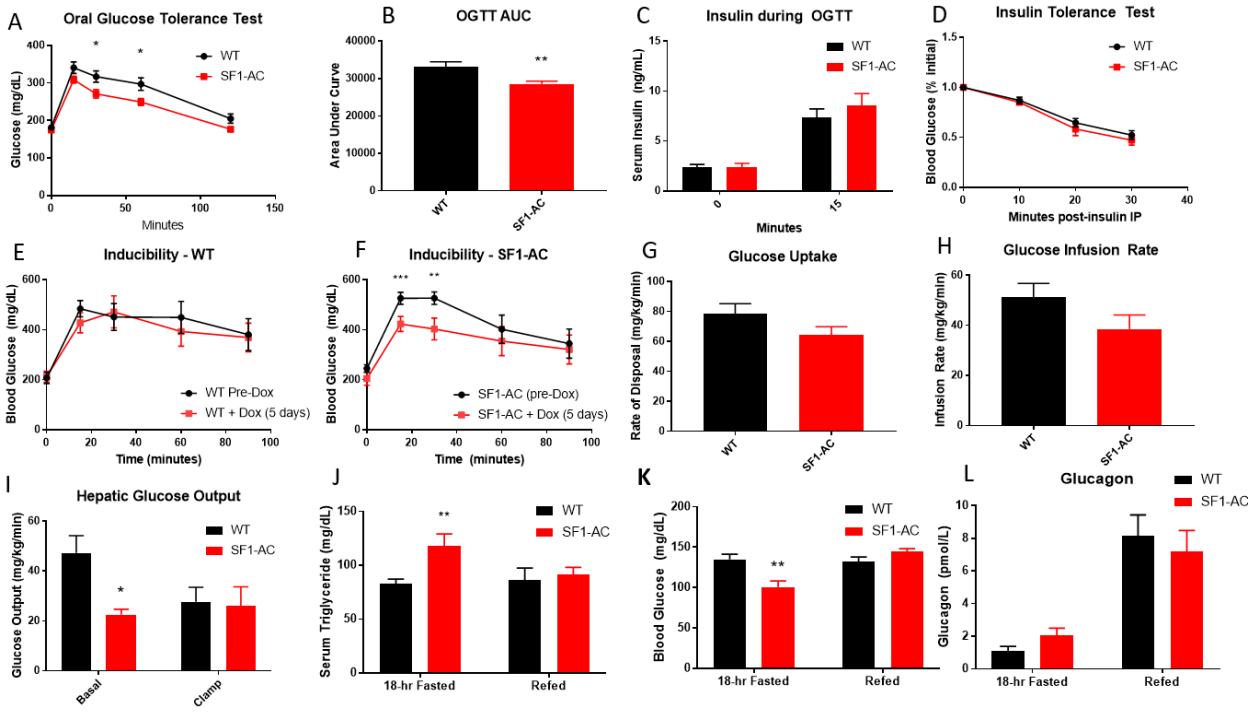

Figure 3.4: SF1-AC mice have improved glucose tolerance without altered insulin resistance. In HFD-fed WT and SF1-AC mice, glucose tolerance (2.5g/kg, **(A-C)**) and insulin tolerance (0.75u/kg,**(D)**) were analyzed. A separate cohort of animals were provided high fat diet without dox for 8 weeks, to examine whether HFD-induced glucose intolerance could be reversed. Glucose tolerance tests (2.5 g/kg) were administered before and 5 days after animals were switched to HFD-dox. Paired responses of WT **(E)** and SF1-AC **(F)** are shown. **(G-I)** Hyperinsulinemic-euglycemic clamps were used to assay changes in insulin sensitivity. Glucose uptake **(G)**, glucose infusion rate **(H)**, and hepatic glucose output **(I)**, are unchanged during the clamp. However, basal hepatic glucose output **(I)** is altered. Serum triglyceride **(J)**, glucose **(K)**, and glucagon **(L)** are shown in 18-hr fasted and refed conditions.

Figure 3.5

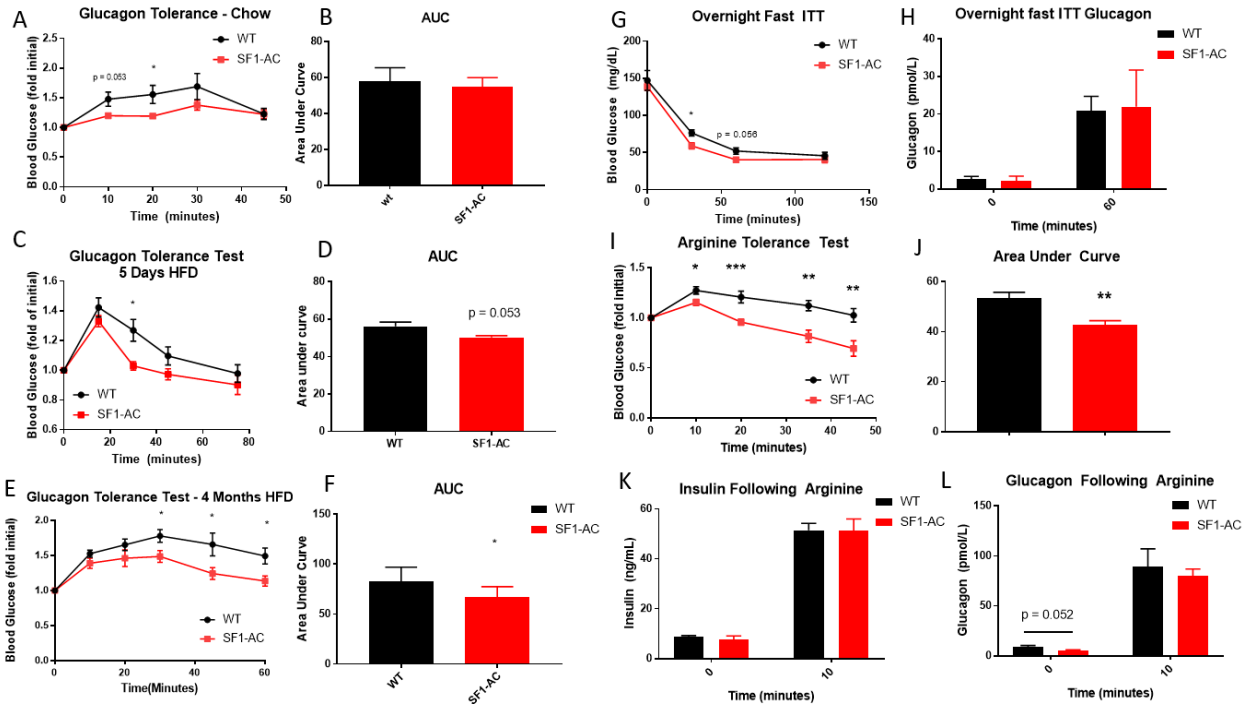

<u>Figure 3.5:</u> Glucagon sensitivity is reduced in SF1-AC mice. Glucagon tolerance was assayed in chow-fed (120 ug/kg, **(A&B)**), 5-days HFD-fed (60 ug/kg, **(C&D)**), and 4-month HFD-fed (120 ug/kg, **(E&F)**) WT and SF1-AC mice. To assay endogenous glucagon action, HFD-fed WT and SF1-AC animals were fasted overnight (20 hrs) before an intraperitoneal insulin injection (1.5 u/kg); blood glucose **(G)** and glucagon secretion **(H)** were monitored. To further demonstrate that endogenous glucagon action is impaired, HFD-fed WT and SF1-AC mice were fasted for two hours prior to an intraperitoneal arginine injection (2g/kg), and blood glucose **(I-J)**, insulin secretion **(K)**, and glucagon secretion **(L)** were monitored during the assay.

Figure 3.6

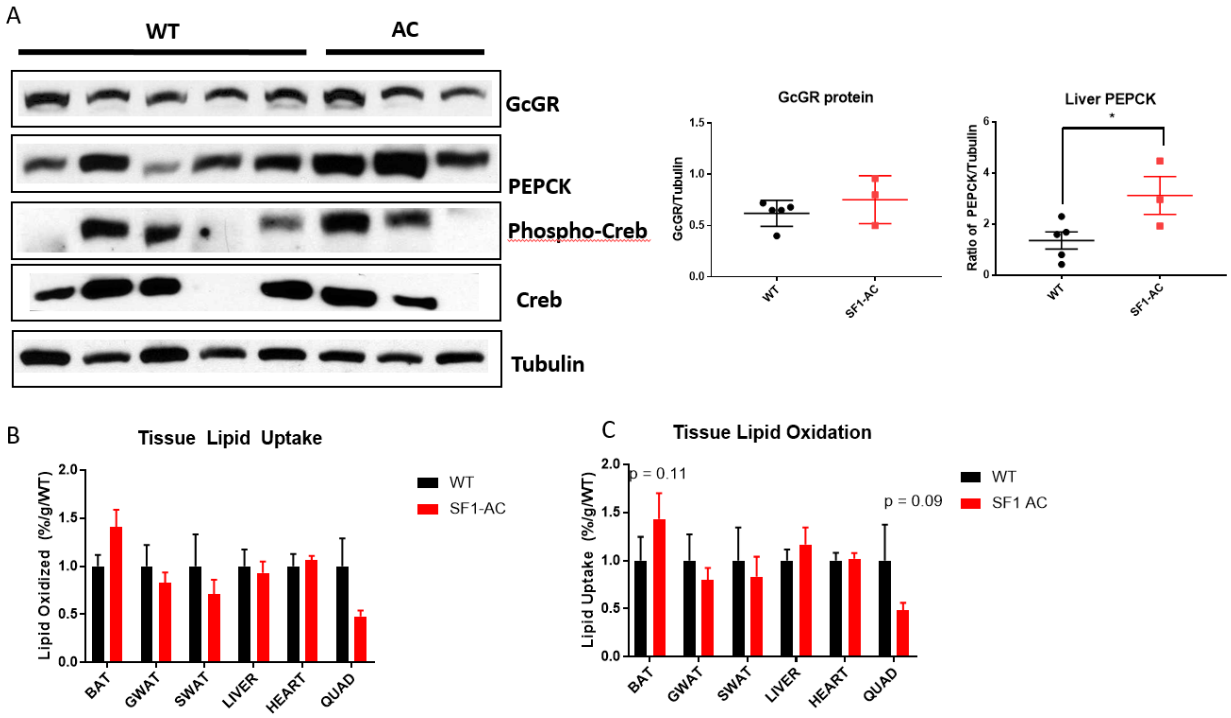

Figure 3.6: Hepatic glucagon signaling and lipid metabolism are unaltered in SF1-AC animals. Glucagon receptor protein and PEPCK protein were analyzed by Western Blot **(A)**. Quantifications are shown to the right. To analyze whole-body lipid metabolism, HFD-fed WT and SF1-AC animals were injected with ^{3}H-labeled triolein, and tissues were analyzed for lipid oxidation **(B)** and lipid uptake **(C)**.

Supplemental Figure 3.1

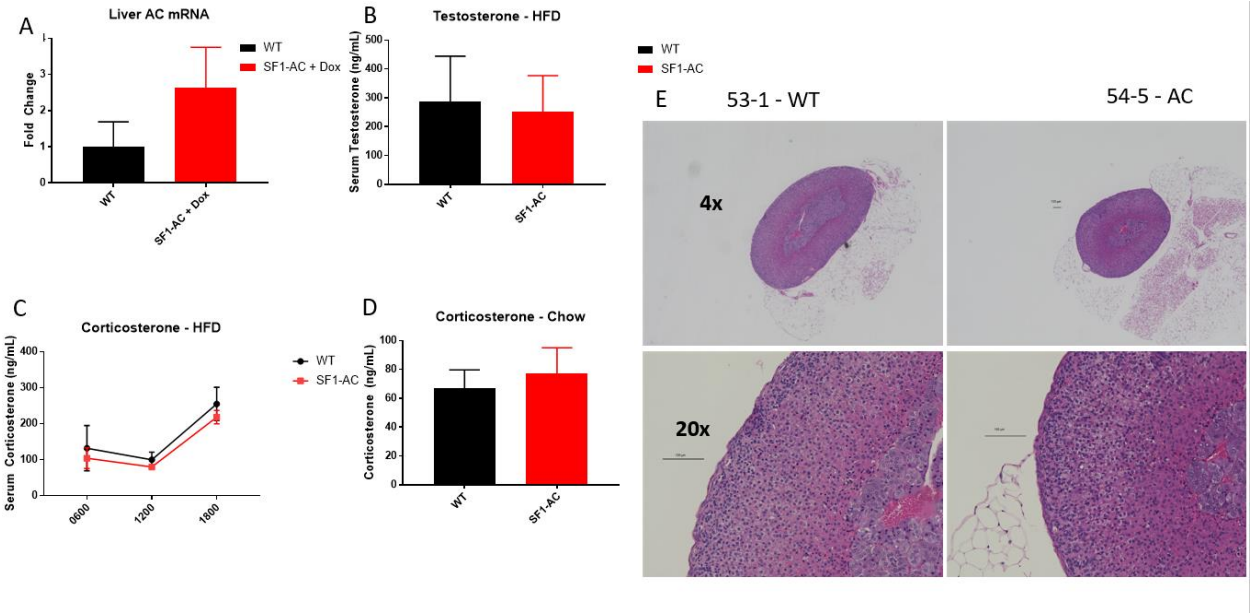

<u>Supplemental Figure 3.1</u>: SF1-AC animals do not have altered adrenal or testicular hormone secretion. Expression of AC is not changed in SF1-AC animals in liver **(A)**. Despite increases in AC expression in testes and adrenals, testosterone **(B)** and corticosterone **(C-D)** are unchanged in SF1-AC animals. Representative adrenal H&E staining is shown in **(E)**.

Supplemental Figure 3.2

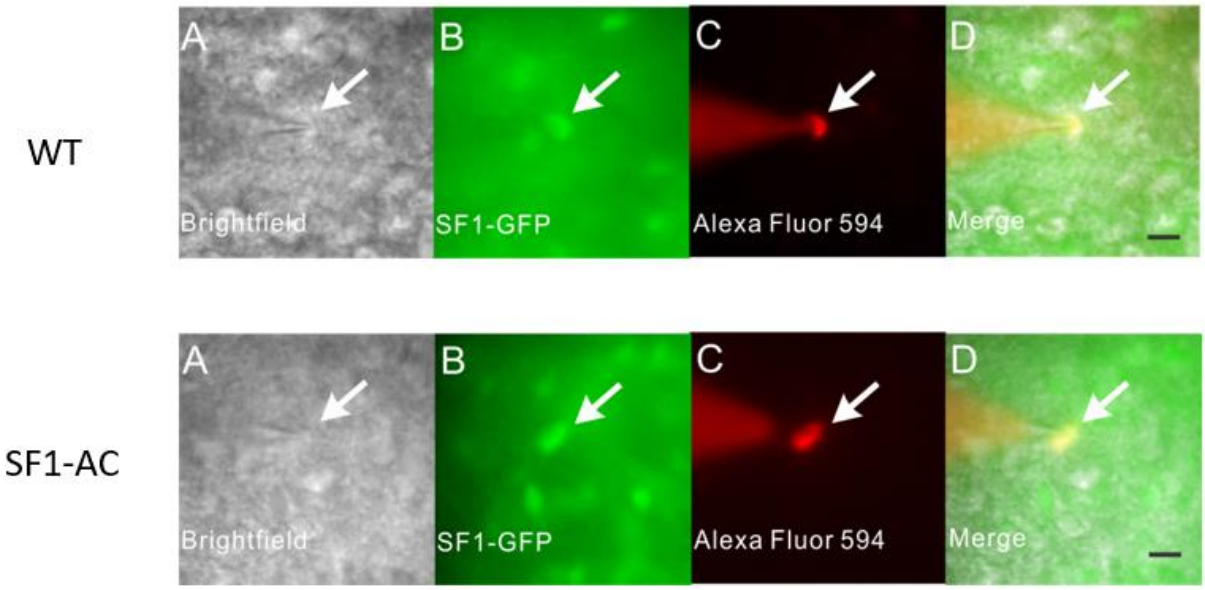

<u>Supplemental Figure 3.2:</u> Demonstration of electrophysiology technique. (A) Brightfield, **(B)** GFP, and **(C)** Alexa 594 illumination of the same neurons in WT (above) and SF1-AC animals (below). Scale bar is 50 µm.

Supplemental Figure 3.3

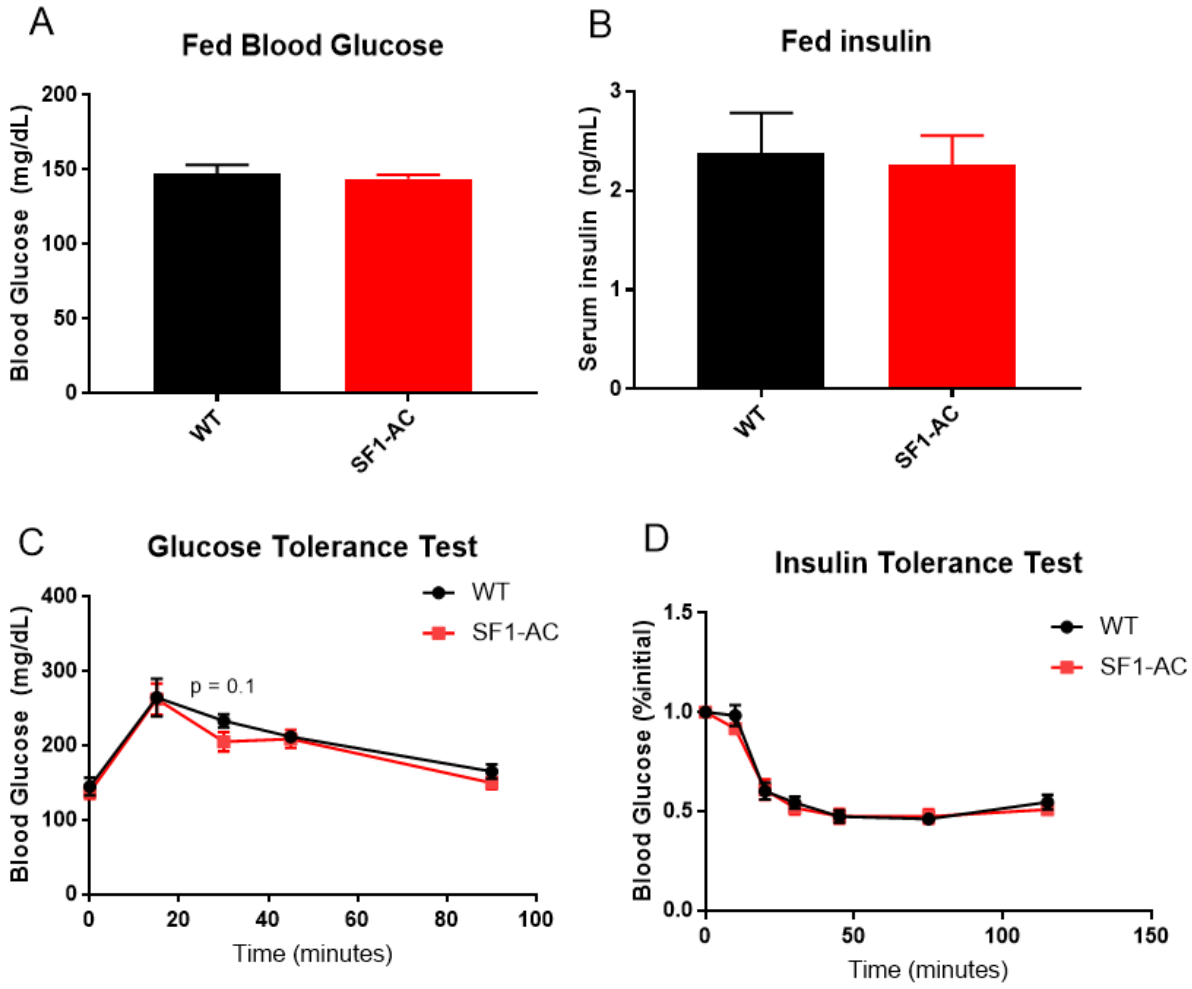

<u>Supplemental Figure 3.3:</u> Glucose tolerance is unchanged in chow-fed SF1-AC animals. Random-fed glucose **(A)** and insulin **(B)** were taken from chow-fed WT and SF1-AC animals. Glucose tolerance tests (2.5 g/kg, **(C)**) and insulin tolerance tests (0.75 u/kg, **(D)**) were performed.

Supplemental Figure 3.4

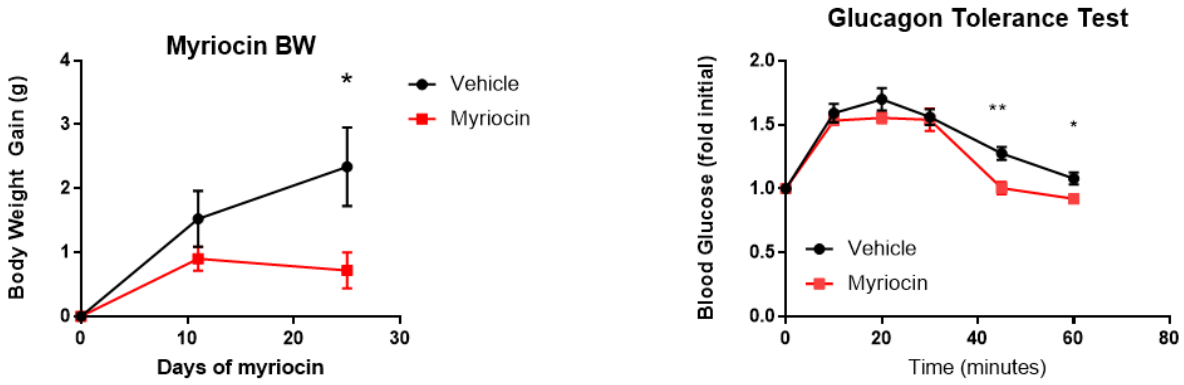

<u>Supplemental Figure 3.4:</u> Demonstration of glucagon tolerance test kinetics in a model of improved insulin sensitivity. As a demonstration of the kinetics of a glucagon tolerance test in a model of improved insulin sensitivity, mice were fed high fat diet for 5 months, before animals were injected with myriocin (0.3 mg/kg) or vehicle (PBS and MeOH) every other day for 25 days. As expected, myriocin reduced body weight gain from HFD feeding **(A)**. On the 25th day, animals were fasted for 1 hour before glucagon (120 ug/kg) was injected and blood glucose **(B)** was monitored.

Supplemental Figure 3.5

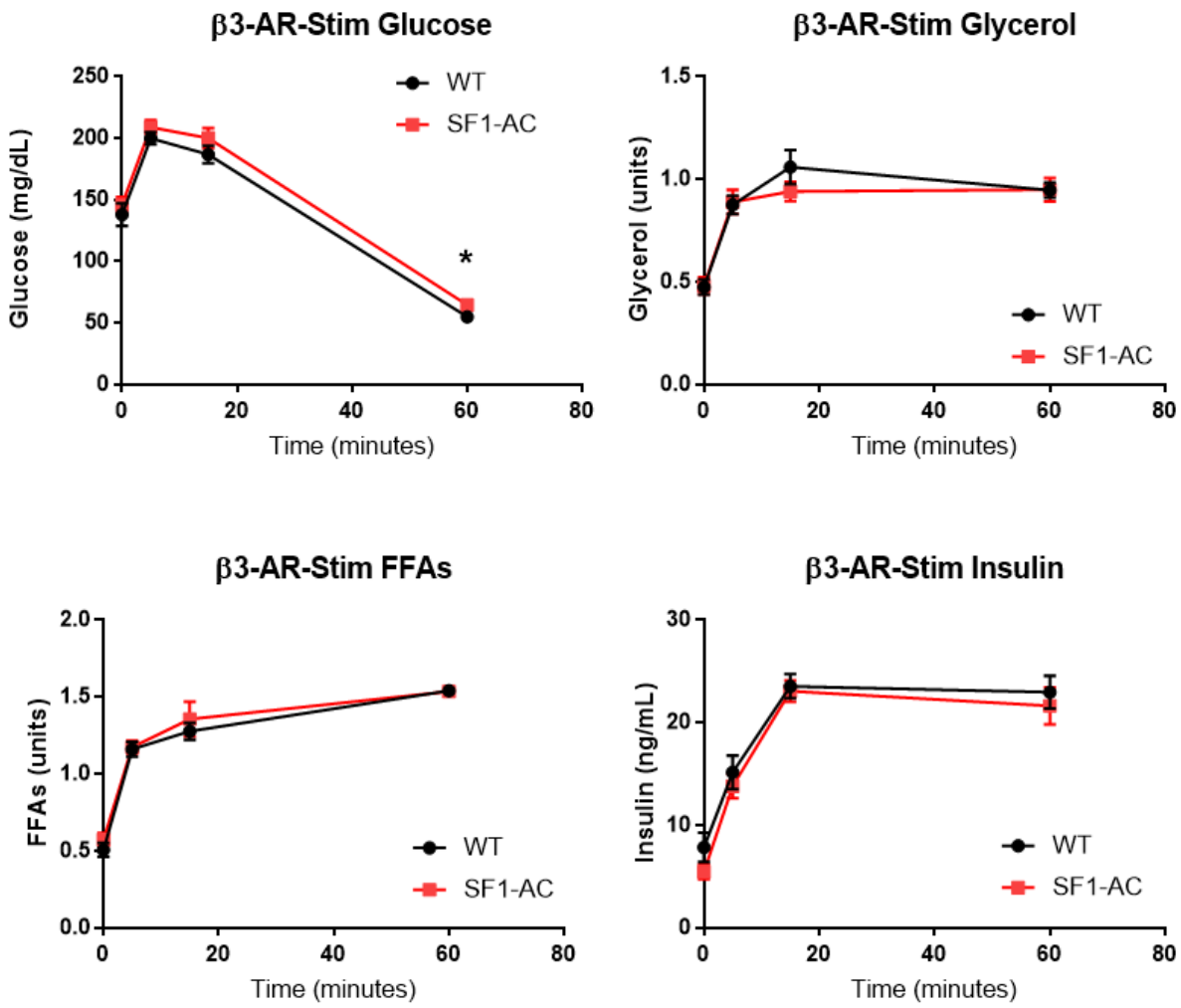

<u>Supplemental Figure 3.5:</u> Adipose tissue β3-adrengergic receptor signaling is unaltered. HFD-fed WT and SF1-AC animals were injected with CL-316,243 (1.5 mg/kg) immediately following removal of food. Blood glucose **(A)**, serum glycerol **(B)**, serum free fatty acids **(C)**, and serum insulin **(D)** were assayed during the experiment.

Chapter 4

A blueprint for the future study of sphingolipids in hypothalamic regulation of body weight and glucose homeostasis

Introduction

As discussed in **Chapters 1-3**, there is a growing body of literature demonstrating a role for sphingolipids in the hypothalamic control of body weight and glucose metabolism. Due to the novelty of the field, numerous gaps in our knowledge remain: which sphingolipids are important? Which cells in the hypothalamus are sensitive to altered sphingolipid content? Are cells other than neurons (such as glia) involved in hypothalamic sensing of sphingolipid content?

To answer these questions, we have made numerous genetic mouse models of altered sphingolipid metabolism. Using previously generated constitutive and inducible *cre* recombinase, loxP-flanked enzymes and receptors, rosa26-rtTA, and TRE-driven alleles, we have interrogated sphingolipid metabolism in multiple cell types with a variety of tools. The preliminary data discussed below comprise a broad blueprint of where sphingolipid metabolism is important positionally in the hypothalamus, as well as which aspects of sphingolipid metabolism and signaling are important in the dysregulation of body weight and glucose homeostasis in obesity.

Methods

Animals. For these studies, all animals were bred to a C57Bl/6J background. All genetic alleles were previously generated and reported: tre-mitoNEET[92], GFAP-CreER[96], constitutive GFAP-cre[97], loxP-flanked GCS[70], POMC-CreER[98], AgRP-CreER[99], loxP-flanked S1PR1[100], AgRP IRES-cre[101], POMC-cre[102]. For tre-driven gene expression, all animals were provided doxycycline (600 mg/kg) in

chow or high fat-high sucrose diet (HFD) as indicated. Body composition was measured by NMR (Bruker, Millerica, MA, USA). All animals were kept on a standard 12-hr light:dark cycle, and all manipulations were done during the light cycle. All control (WT) animals were littermate controls of the experimental animals.

Oral glucose tolerance tests. For oral glucose tolerance tests (OGTT), animals were placed in a procedure room to acclimate and fasted for 5 hours. Glucose (2.5 g/kg) was injected to the stomach via oral gavage at the end of the fast, and blood glucose was measured at the indicated points. To measure glucose-stimulated insulin secretion, serum was drawn before and 15 minutes after a glucose bolus.

Insulin tolerance tests. Unless otherwise noted, animals were placed in a procedure room to acclimate and fasted for 3 hours. Insulin was prepared in PBS with a few mg of BSA as a carrier, and injected at 1.5 U/kg intraperitoneally and blood glucose was measured at the indicated points.

Serum insulin and glucagon measurement. For all serum insulin measurements, a commercially available insulin ELISA (Crystal Chem, Elk Grove Village, IL, USA) was used according to manufacturer instructions. For serum glucagon measurements, a commercially available glucagon ELISA (Mercodia, Uppsala, Sweden) was used according to manufacturer instructions.

Hyperglycemic clamps. Hyperglycemic clamps were performed on jugular-catheterized animals which were prepared as in **Chapter 3**. Briefly, animals were fasted for five hours in the morning. Next, glucose was infused to achieve a blood glucose of ~250 mg/dL. Blood was drawn at the indicated time points, and insulin was measured by insulin ELISA.

Tamoxifen administration. For POMC-CreER mice, tamoxifen (150 μg/kg) was injected for five consecutive days before studies began. For AgRP-CreER mice, tamoxifen (150 μg/kg) was injected following an overnight fast; animals then received at least a two day break of normal feeding before

being fasted and injected again, for a total of 5 injections. For GFAP-CreER mice, tamoxifen (150 μg/kg) was injected at the indicated time points.

Streptozotocin-induced diabetes. Two doses of streptozotocin (100 mg/kg) were injected following an overnight fast to induce moderate insulin-deficient diabetes in POMC AC mice.

Arginine tolerance test. To assay whether pancreatic function was intact in GFAP-mitoNEET animals, arginine (2 g/kg) was injected into 2-hr fasted animals. Glucagon and insulin were measured by ELISA at 0 and 15 minutes following the injection.

Gene expression. Tissues were harvested, dissected as needed, and snap frozen in liquid nitrogen. To extract mRNA, tissues were homogenized in Trizol and extracted according to manufacturer specifications (Thermo Fisher, Waltham, MA, USA). mRNA concentration was measured with a spectrophotometer, and cDNA was created using a kit according to manufacturer instructions (Thermo Fisher). Gene expression was assayed using the primers described in **Chapter 2**.

Results & Discussion

Ablation of glucosylceramide synthase in astrocytes alters body weight regulation with minimal effects in POMC neurons and uncertain effects in AgRP neurons.

To study the importance of glucosylceramides in hypothalamic body weight regulation (see **Chapter 1**), we bred previously generated animals harboring glucosylceramide synthase (GCS) loxP-flanked alleles with animals expressing tamoxifen-inducible *cre* in GFAP-expressing cells. The resulting animals (termed GFAP GCS^{KO}) will ablate expression of GCS in astrocytes upon administration of tamoxifen. To understand whether ablation of GCS in astrocytes could prevent high fat diet-induced obesity, we injected tamoxifen for five consecutive days before providing high fat diet, allowing us to examine whether glucosylceramide accumulation or production in astrocytes plays a role in early diet-

induced weight gain. However, during the 10 weeks of HFD feeding GFAP GCS^{KO} animals did not demonstrate any difference in body weight (**Figure 4.1A**). However, as GFAP-cre may not be fully expressed under chow fed conditions[103], we repeated this experiment with a spaced tamoxifen regimen, where HFD and tamoxifen were administered concurrently (as depicted in **Figure 4.1B**). Using this protocol, tamoxifen administration occurs concurrently (rather than prior to) HFD-mediated activation of the GFAP promoter in astrocytes, which may allow for more robust expression of *creER* and subsequent excision of the loxP-flanked GCS allele. In this paradigm, we noted a striking decrease in body weight in animals with GCS deleted from GFAP-expressing cells (**Figure 4.1B**). Furthermore, we analyzed food intake after the divergence in body weight, and noted a substantial decrease in feed efficiency and increase in food intake per body weight, suggesting a possible difference in energy expenditure (**Figure 4.1C-D**). In agreement, hypothalamic gene expression demonstrated a significant increase in expression of the orexigenic peptide *Agrp* in GFAP GCS^{KO} animals, as well as a surprising increase in *Il-6* expression (**Figure 4.1E**). Interestingly, when we examined the brains and livers of the GFAP GCS^{KO} animals for excision of GCS, GCS excision was only detected in the liver, but not in the brain (**Figure 4.1F**). This is surprising, as we had expected to find plentiful excision in the brain (where GFAP-expressing astrocytes exist and robustly express GFAP following high fat feeding) with minimal excision in the liver, where scarce hepatic stellate cells that may express GFAP exist, particularly in a context where the liver has not been challenged with an exogenous stress other than HFD. Thus, these studies raise the question of whether the effects we see of GCS ablation is due to ablation of GCS in astrocytes in the brain or ablation of GCS in hepatic stellate cells.

Together, these preliminary findings suggest a strong effect of glucosylceramide accumulation and synthesis in astrocytes (or, perhaps, hepatic stellate cells) in mediating high fat diet-induced weight gain. To further understand the mechanism behind this, GFAP GCS^{KO} animals should be evaluated in metabolic chambers to understand the driver of the changes in body weight: is this phenotype energy-

expenditure related, food intake-related, or a combination of the two? The preliminary data in **Figure 4.1C-D** suggest that the phenotype will be related to increased energy expenditure. It will also be imperative to determine whether ablation of GCS in astrocytes also has effects on glucose homeostasis; due to the meaningful change in body weight that we observed in the second paradigm (**Figure 4.1B**), we elected not to carry out measurements of glucose tolerance or insulin sensitivity in this cohort.

Finally, to dissect whether the phenotype of GFAP GCS^{KO} animals is mediated by GCS ablation in astrocytes or hepatic stellate cells, we plan to cross the loxP-flanked GCS allele with a novel lecithin:retinol acyltransferase (LRAT) promoter-driven rtTA and previously generated tre-cre alleles. LRAT is expressed exclusively by hepatic stellate cells[104]; this novel LRAT-rtTA (produced by the lab of Philip Scherer) will allow for ablation of GCS exclusively in hepatic stellate cells, allowing us to determine whether the metabolic effects in the GFAP GCS^{KO} animals are due to GCS ablation in astrocytes or in hepatic stellate cells.

Ablation of glucosylceramide synthase results in minimal effects in POMC neurons and uncertain effects in AgRP neurons.

As others have demonstrated that GCS inhibition in the hypothalamus has potent effects on body weight, we attempted to genetically manipulate two arcuate neuron populations, those that express AgRP and those that express POMC. AgRP and POMC neurons are well-characterized as vital players in neuronal body weight and glucose homeostasis[reviewed in 105]. As above, previously-generated tamoxifen inducible *cre* lines were bred with loxP-flanked GCS lines, yielding AgRP GCS^{KO} and POMC GCS^{KO} animals. To test whether accumulation of glucosylceramides in POMC neurons contributes to HFD-induced weight gain, we ablated GCS expression using a previously reported tamoxifen injection protocol of five daily tamoxifen injections[98]. In both chow and high fat diet-fed conditions, we did not detect any alterations in body weight when GCS is ablated in POMC neurons (**Figure 4.2A-B**).

Interestingly, we did note a significant decrease in glucose tolerance without significantly altered insulin sensitivity on HFD, although this effect was relatively minor (**Figure 4.2C-D**). As these effects were insignificant, we elected not to continue phenotyping these animals.

As AgRP neurons are the better appreciated body weight regulating neurons, we were interested to see the effects of GCS ablation in AgRP neurons; unfortunately, we discovered that AgRP GCS^{KO} mice demonstrated a significantly lower body weight prior to any tamoxifen injections, confounding any inferences of the effect of ablating GCS in AgRP neurons (**Figure 4.2E**). This phenomenon was strong enough that animals could be reliably assigned a genotype by visual inspection alone, with following confirmation by PCR with 100% success rate (data not shown). This finding remains wholly unexplained, as we and others have not noted any change in body weight in animals carrying either the homozygous floxed alleles or the tamoxifen inducible AgRP *cre* allele[99].

In summary, although others have shown that inhibition of GCS in the hypothalamus has potent effects on body weight[51], our data suggests that these effects are mediated outside of POMC neurons; we cannot rule out effects in AgRP neurons (which are well-known for their effects on body weight regulation) due to the robust body weight phenotype in these animals prior to administration of tamoxifen. However, in combination with our previously described data in GFAP GCS^{KO} animals, we would speculate that the effects of GCS inhibition on body weight are mediated through astrocytes and not hypothalamic neurons.

Ablation of sphingosine-1-phosphate receptor 1 in AgRP-expressing neurons reduces HFD-induced weight gain, but does not alter weight gain when ablated in POMC- or GFAP-expressing cells.

Previous studies have demonstrated important roles for sphingosine-1-phosphate (S1P) signaling in hypothalamic control of body weight. Others have found that intracerebroventricular S1P injections causes marked reductions in food intake and increases in thermogenesis by driving STAT3

signaling [106]; in that study, the authors had postulated that sphingosine-1-phosphate receptor 1 (S1PR1) receptors in POMC neurons mediated these effects. In the hypothalamus, S1PR1 is expressed most robustly in arcuate, ventromedial, and dorsomedial hypothalamus[106]; additionally, expression of S1PR1 seems to be restricted to neurons, with S1PR1 demonstrating minimal colocalization with GFAP.

As we have access to the genetic tools to inducibly ablate S1PR1 in POMC neurons, AgRP neurons, or astrocytes, we decided to investigate whether S1P signaling in the hypothalamus exerts its effects through these neuronal or astrocytic populations. To study the importance of S1P in hypothalamic body weight regulation, we utilized previously generated tamoxifen-inducible POMC-*creER,* AgRP-*creER*, or GFAP-*creER* mice bred with previously generated loxP-flanked S1PR1 animals. These animals allow for tamoxifen-inducible ablation of S1PR1 in the cells of our choice. Although the previous work had suggested that S1PR1 receptors in POMC neurons mediated the effects of intracerebroventricular S1P injections, we were surprised to find that tamoxifen-induced ablation of S1PR1 in POMC neurons caused no change in body weight on HFD (**Figure 4.3A**). Furthermore, no changes in 24-hour fasted rebound food intake were noted in these animals (**Figure 4.3B**). As POMC neurons also play a significant role in glucose homeostasis, we were also surprised to find that S1PR1 ablation in POMC neurons did not alter glucose homeostasis, with $S1PR1^{KO}$ animals demonstrating identical glucose tolerance to wild-type counterparts (**Figure 4.3C**). Similarly, we did not note any changes in body weight regulation when knocking out S1PR1 in GFAP-expressing cells (**Figure 4.3D**), in agreement with the previous observation that S1PR1 and GFAP do not colocalize in the hypothalamus.

Although the previous report had indicated that POMC S1PR1 receptors may be responsible for the effects of S1P on hypothalamic body weight control, we hypothesized that those effects may be mediated by AgRP neurons in the arcuate hypothalamus. Indeed, when S1PR1 was inducibly deleted in AgRP neurons, the resulting AgRP S1PR1 KO mice were rendered highly resistant to HFD-induced obesity (**Figure 4.4A**). Despite an approximate difference of 15g in body weight by the end of the study, AgRP

S1PR1 KO animals demonstrated similar food intake to WT animals (**Figure 4.4B**); accordingly, AgRP S1PR1 KO mice demonstrated a trend to increased food intake when expressed as a percentage of body weight (**Figure 4.4C**). Additionally, rebound feeding (following a 24-hour fast) was unchanged in AgRP S1PR1 KO animals in both absolute and body-weight-relative terms (**Figure 4.4D**). The lack of difference in food intake despite significantly decreased body weight suggests that alterations in energy expenditure may explain the differences in body weight that developed during the study. However, as these food intake studies were conducted at the end of the body weight study (after significant body divergence), it is possible that differences in food intake during the divergence in body weight is responsible for the phenotype rather than changes in energy expenditure. Metabolic cage studies in weight matched cohorts are warranted to discern between these two explanations.

Regardless, these findings contrast starkly with those previously reported when S1P is injected directly into the brains of rats (as previously reported) in a number of important ways. First, the previous work had shown that S1P acted in the hypothalamus to cause decreased food intake and body weight. Conversely, we would expect that removal of S1PR1 in hypothalamic neurons would cause weight gain; this was not found to be the case, as knocking out S1PR1 in AgRP neurons also caused weight loss. It is plausible that this discrepancy may be mediated by neuronal populations outside of the ones studied here, which may have an opposite response to S1P that is strong enough to override that of AgRP neurons. Additionally, the previous work had implicated S1PR1 in POMC neurons as a key mediator S1P's body weight regulation, whereas our work would suggest an important role for S1P signaling in AgRP neurons, but not POMC neurons.

Overexpression of mitoNEET in astrocytes decreases body weight and impairs glucose tolerance by reducing insulin secretion

It has been recently demonstrated that lipolysis in the hypothalamus and hippocampus serves a vital role in body weight regulation in studies which modulate lipoprotein lipase activity in the brain[50, 107]. We were interested in whether these effects may be mediated by β-oxidation in neurons of the hypothalamus. To modulate tissue-specific β-oxidation, our group has previously generated a construct to overexpress mitoNEET in a tet-controlled manner. MitoNEET is able to reduce β-oxidation by inhibiting mitochondrial iron transport[92, 108]. Although others (personal communication from K. Williams) have found little role for β-oxidation in body weight and glucose regulation in POMC neurons, we were curious whether there was a role for β-oxidation in the regulation of glucose and body weight by astrocytes. To answer this, we bred previously generated GFAP-*cre*, rosa26-rtTA, and tre-mitoNEET animals to yield animals that overexpress mitoNEET in astrocytes upon the administration of doxycycline in the diet (GFAP-mitoNEET). When challenged with high fat diet, GFAP-mitoNEET mice gained less weight that wild type littermates (**Figure 4.5A**). In a second cohort of animals, we assayed glucose homeostasis in weight-matched mice and found a surprising decrement in glucose tolerance (**Figure 4.5B**). This worsening of glucose tolerance was noted to occur along with a greatly attenuated (but not statistically significant) insulin secretion in response to an oral glucose bolus (**Figure 4.5C**). As may be expected in animals secreting less insulin, GFAP-mitoNEET mice were also more insulin sensitive than their wild-type counterparts when assayed by an insulin tolerance test (**Figure 4.5D**). We next asked whether the decrease in insulin secretion was due to reduced pancreatic function, or a *bona fide* decrease in sensitivity to increased circulating glucose. To test this, we injected arginine, which will completely depolarize (and degranulate) α- and β-cells of the pancreas. Interestingly, we did not note any significant changes in insulin or glucagon secretion following arginine, demonstrating an intact endocrine pancreas and islets (**Figure 4.5E-F**). Finally, we attempted the gold standard of insulin secretion assays, the hyperglycemic clamp, where animals are infused with supraphysiologic glucose and insulin secretion is monitored. Unfortunately, we were not able to demonstrate an increase in serum

insulin in either GFAP-mitoNEET or control animals despite the infusion of large amounts of glucose; however, in agreement with our earlier data, GFAP-mitoNEET mice demonstrated lower serum insulin during the course of the study (**Figure 4.5G**). Thus, our preliminary data indicates that mitoNEET overexpression in astrocytes serves to blunt weight gain on HFD and reduces glucose tolerance by impaired insulin secretion. It is logical to assume that the decreased insulin secretion in response to a glucose bolus may, over a chronic high fat diet feeding, cause reduced body weight gain, owing to insulin's well-recognized role in promoting adipogenesis. Regardless, further study is required to dissect the mechanism by which body weight gain is altered in GFAP-mitoNEET animals.

Interestingly, alterations of insulin secretion by perturbing astrocyte function have recently been reported: others have found that ablation of insulin receptor in astrocytes can decrease insulin secretion following an oral glucose bolus, leading to glucose intolerance[109]. It was postulated that these changes were due to altered glucose sensing by hypothalamic astrocytes following insulin receptor ablation. Our data demonstrate further evidence that astrocyte nutrient sensing is important in glycemic regulation following meals, as well as in regulating body weight.

Reduction of ceramide content in AgRP neurons does not alter body weight or glucose homeostasis, while reducing ceramide content in POMC neurons alters body weight in females and streptozotocin-induced glucose handling in males.

As we have previously demonstrated (**Chapter 3**), ceramide accumulation during high fat feeding plays a vital role in altering hypothalamic control of glucose homeostasis. Indeed, as we had shown that VMH neurons respond to ceramide accumulation, we became curious whether this was also true of neurons within the arcuate hypothalamus, particularly the well-characterized AgRP and POMC neurons. To answer this, we bred the previously generated rosa26-rtTA and tre-AC mice with constitutive AgRP- and POMC-driven *cre* animals to generate dox-inducible tissue-specific

overexpression of AC (and reduction of ceramide) in AgRP or POMC neurons, respectively. As ceramide accumulation in hypothalamic neurons has been shown to result in increased weight gain (reviewed in **Chapter 1**), we predicted that lowering ceramides in AgRP neurons would result in reduced body weight in response to HFD. However, in AgRP AC animals, we noted no differences in body weight or body composition after high fat feeding (**Figure 4.6A-B**). Additionally, we did not detect differences in glucose tolerance in AgRP AC animals (**Figure 4.6C**).

Although we found no effect of AC overexpression in AgRP neurons, we were interested to determine whether POMC neurons were instead responsible for the deleterious effects of ceramides on central body weight and glucose regulation. Interestingly, we discovered a sexually dimorphic phenotype in the response to AC overexpression in POMC neurons. In male mice, we noted no differences in body weight gain following high fat diet (**Figure 4.7A**). Additionally, oral glucose tolerance and insulin sensitivity were unchanged following high fat feeding (**Figure 4.7B-C**). To further determine whether ceramide accumulation in POMC neurons were important in the maintenance of glucose homeostasis, we challenged a cohort of animals with streptozotocin to induce an insulin deficient state. Interestingly, we did note a significant improvement in glucose homeostasis in a trial of streptozotocin-treated POMC AC males (**Figure 4.7D**). This effect was noted to be independent of insulin and glucagon secretion, as serum insulin was unchanged (and at the low limits of detection) with serum glucagon being unchanged (and higher than normal) during the oral glucose challenge (**Figure 4.7E-F**). Although male POMC AC mice did not have any detectable differences after high fat feeding, in females we noted a dramatic increase in the body weight of POMC AC animals (**Figure 4.8A**). Despite the large difference in body weight, no alterations in glucose tolerance were noted (**Figure 4.8B**) due to the pronounced compensation of increased insulin secretion during the oral glucose challenge (**Figure 4.8C**). However, POMC AC females were less insulin sensitive than their WT counterparts, as anticipated by their greatly increased body weight (**Figure 4.8D**). This sexually dimorphic phenotype was surprising in two respects.

First, it was surprising that there was no effect of AC overexpression in males, as most of the pharmacological ceramide inhibition studies (reviewed in **Chapter 1**) which showed an effect on body weight were done in males. Second, it was surprising that AC overexpression in females led to increased body weight and blunted insulin sensitivity; other studies had shown that reducing ceramides in the hypothalamus should be salutary for both weight gain and glucose homeostasis, whereas these studies suggest the opposite conclusion.

To test whether the effects of ceramide depletion in the arcuate hypothalamus of male mice required actions on both POMC and AgRP neurons, we created a mouse model overexpressing acid ceramidase in both POMC and AgRP neurons by breeding animals containing both POMC-*cre* and AgRP-*cre* to the previously described Rosa26-rtTA and tre-AC animals (mice termed Double AC). When challenged with high fat diet for four months, Double AC animals did not display any improvements in body weight gain (**Figure 4.9A**). Furthermore, Double AC animals did not have altered glucose tolerance (**Figure 4.9B**) following the high fat feeding. Finally, to understand whether ceramide accumulation had any role in maintaining the hypothalamic set point following reversal of high fat feeding, we returned these animals to a dox-chow diet after the four month high fat diet period. However, even after a month of chow diet Double AC animals failed to lose weight any faster than wild type littermates (**Figure 4.9C**), thus demonstrating that ceramide accumulation following high fat feeding in arcuate neurons is also not responsible for altering the hypothalamic set-point in obesity.

These data conclusively demonstrate that ceramide accumulation in arcuate neurons plays little role in altering body weight homeostasis in male mouse models. In POMC AC, AgRP AC, or the Double AC mouse models we consistently found no alterations in body weight or body composition across multiple cohorts of mice. Similarly, no role was found for ceramides in these neurons in altering glucose homeostasis, as tested in multiple cohorts. The only phenotypic difference observed was in POMC AC males which were challenged with streptozotocin, which displayed a moderate improvement in glucose

tolerance despite unaltered insulin secretion during the OGTT. The mechanism behind this change remains to be elucidated. However, we did discover a clear role for POMC neuron ceramides in modulating body weight in females. This was surprising, as the importance of a sexual dimorphism in ceramide-mediated effects has not been reported in the literature. Furthermore, the preponderance of data in the literature would suggest that lowering ceramides in the hypothalamus should be protective against HFD-induced weight gain, whereas our data in female mice suggests the opposite. This may relate to the fact that most of the data in the literature has been derived in male mice and not reported in female mice. Furthermore, it is possible that the physiology of sphingolipid accumulation in females is different from that in males; while HFD-fed males have markedly increased ceramide, glucosylceramide, and sphingomyelin in the hypothalamus, HFD-fed females demonstrate decreased levels of these lipids[110]. Thus, it is logical to propose that a sexual dimorphism may exist in the response to ceramide depletion in the hypothalamus in obesity, such that lowering ceramide content in female hypothalami below their baseline levels is deleterious.

Conclusion

The data described above are comprised of a number of manipulations of sphingolipid metabolism in multiple cell types in the hypothalamus. In summary, they describe a vital role for various sphingolipid species in multiple different hypothalamic cell types. Importantly, it appears that many of the effects of sphingolipid accumulation in the hypothalamus occur outside of the well-studied neurons of the arcuate hypothalamus, the POMC and AgRP neurons. This is surprising, as POMC and AgRP neurons are both known to be key players in hypothalamic control of metabolism; it was logical to expect that they would mediate at least some of the effects of ceramide accumulation during obesity on dysregulation of body weight and glucose homeostasis.

Indeed, the strongest and most reproducible effects we observed were when lipid metabolism was altered in astrocytes in the hypothalamus by either ablating glucosylceramide synthesis or overexpressing mitoNEET. This begets the working hypothesis that most of the effects of accumulation of sphingolipids in the hypothalamus are mediated through astrocytes (or other glia), rather than in neurons *per se*. Indeed, the mechanism by which astrocytes exert their effects to alter neuronal control of metabolism is an area of active research; the above data argue that it will be necessary to utilize the tools being developed to study the astrocyte's role in metabolism to truly understand the role of sphingolipids in hypothalamic control of metabolism.

Finally, the discovery that derivatives of ceramide such as S1P and glucosylceramide both have important roles in regulating body weight, while ceramides *per se* seem to lack much role in arcuate control of body weight is somewhat surprising, particularly considering the pharmacological studies outlined in **Chapter 1**. Indeed, our studies show a vital role for S1P signaling in regulating body weight in AgRP neurons, whereas decreasing ceramide content in these same neurons does not demonstrate a potent phenotype.

These data provide an important blueprint for future studies on sphingolipid-mediated changes in neuronal control of metabolism. In summary, it appears that hypothalamic glia should be the target of future studies, while select manipulations of hypothalamic neuronal populations may bear fruit as well.

Figure 4.1

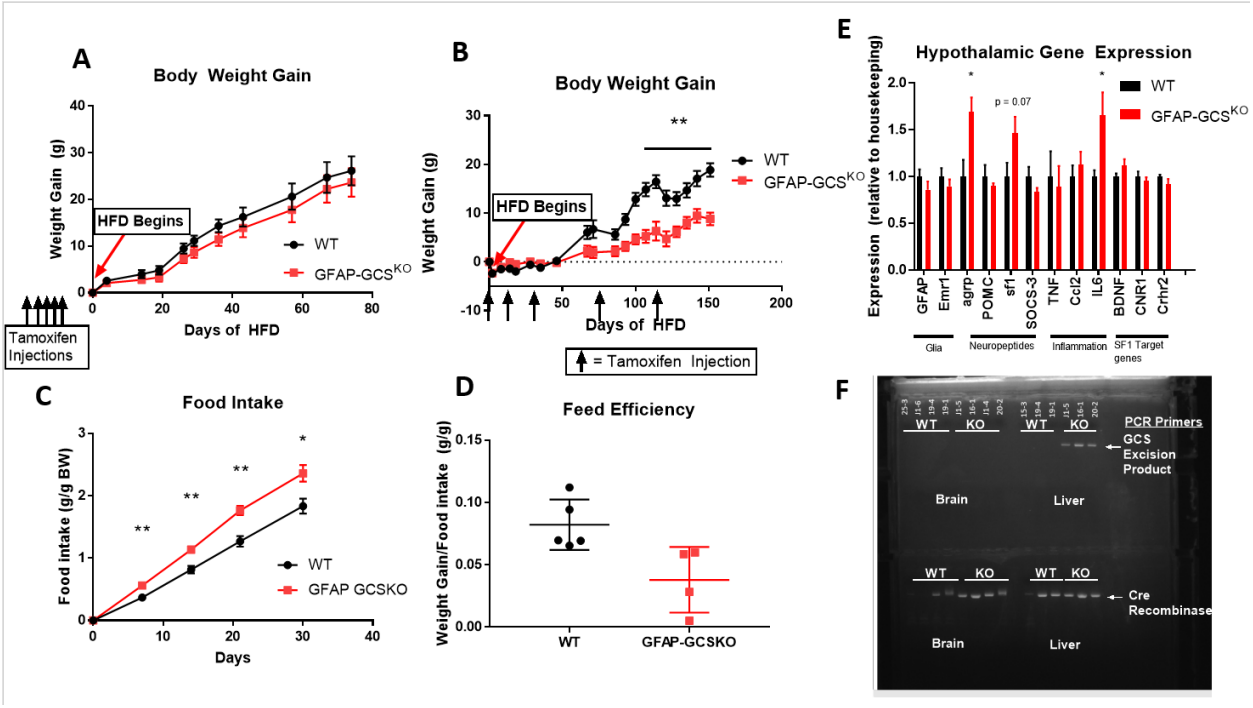

<u>Figure 4.1:</u> Ablation of glucosylceramide synthase in astrocytes causes resistance to HFD-induced weight gain. WT and GFAP GCS^{KO} mice were treated with tamoxifen (150 µg/kg) before HFD and body weight was monitored (A). In a second cohort of animals, WT and GFAP GCS^{KO} mice were treated with tamoxifen before and during HFD feeding (B). Food intake (C) and feed efficiency (D) were monitored at the end of the concurrent tamoxifen-HFD study in (B). Following sacrifice, hypothalamic gene expression was assayed in WT and GFAP GCS^{KO} mice (E). Finally, PCR was carried out on liver and brain to detect the GCS excision product (F). n = 4-5 per group, * $p < 0.05$, ** $p < 0.01$.

Figure 4.2

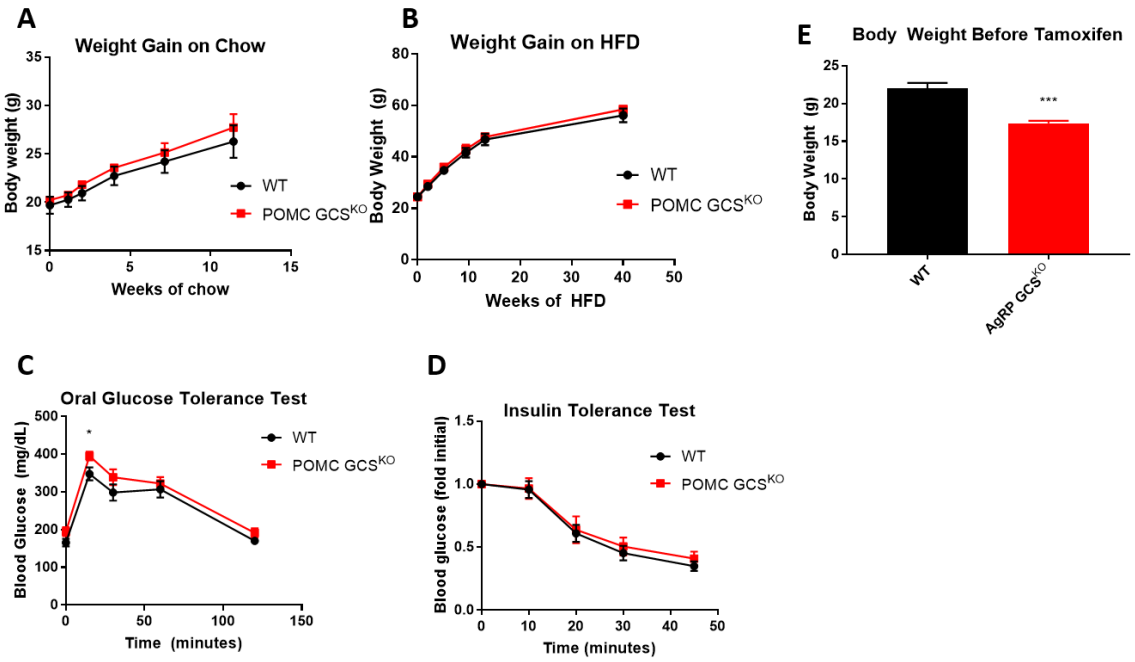

<u>Figure 4.2:</u> Ablation of glucosylceramide synthase in POMC neurons does not alter HFD-induced weight gain or insulin resistance. WT and POMC GCS^{KO} animals were treated with tamoxifen (150 µg/kg) for 5 days prior to chow (A) or HFD (B) administration. Glucose tolerance (C) and insulin tolerance (D) were assayed in the HFD-fed animals. Body weights were measured in WT and AgRP GCS^{KO} prior to tamoxifen administration (E). n ≥ 4 per group, * $p < 0.05$.

Figure 4.3

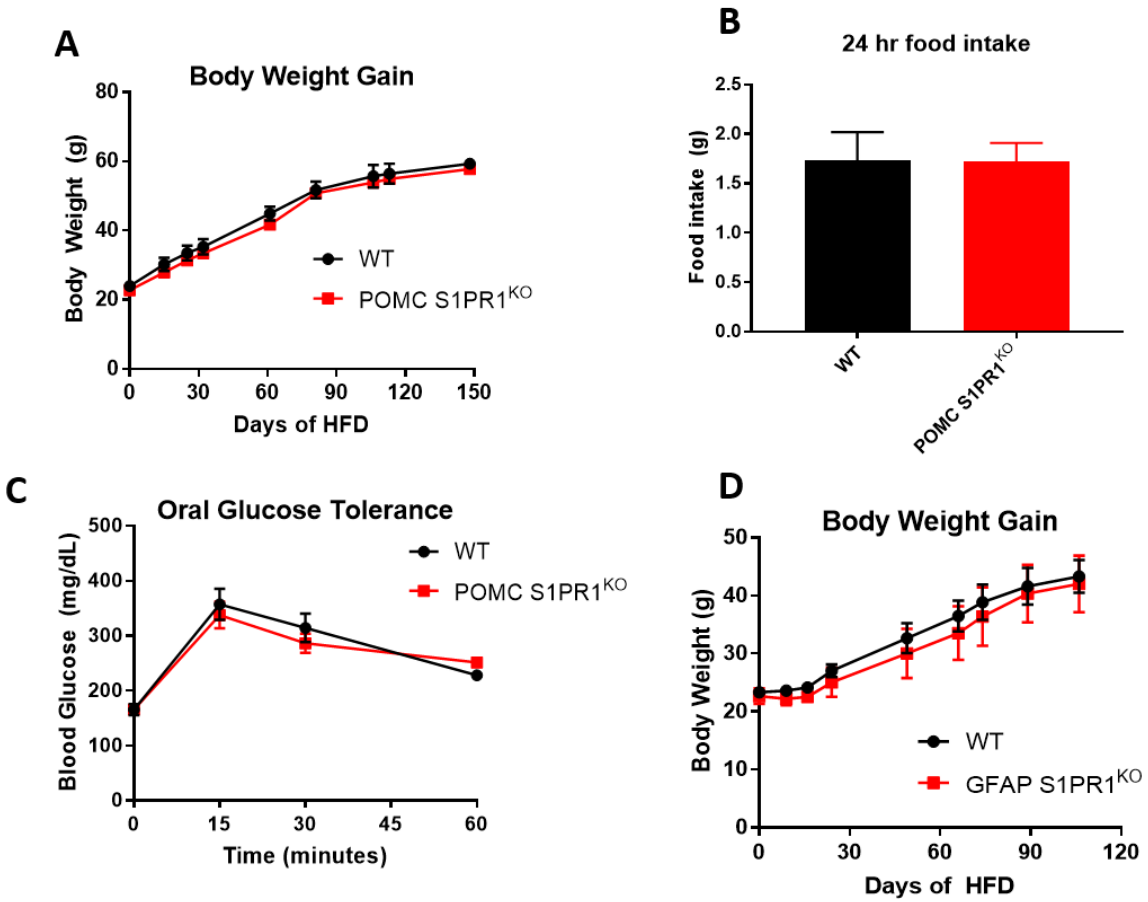

<u>Figure 4.3:</u> Ablation of S1PR1 in POMC neurons or astrocytes does not alter weight gain or insulin sensitivity. WT and POMC S1PR1^{KO} animals were injected with tamoxifen (150 µg/kg) daily for five days before being provided high fat diet and monitoring body weight (A) (n = 5 per group). Following a 24-hr fast, WT and P POMC S1PR1^{KO} were provided food, and food intake was measured over the next 16 hours (B). Oral glucose tolerance was assayed in WT and POMC S1PR1^{KO} during HFD feeding (C). WT and GFAP S1PR1^{KO} mice were provided HFD and given a single tamoxifen injection (150 µg/kg) at day 0 and again at day 49 (D) (n = 3-4 per group).

Figure 4.4

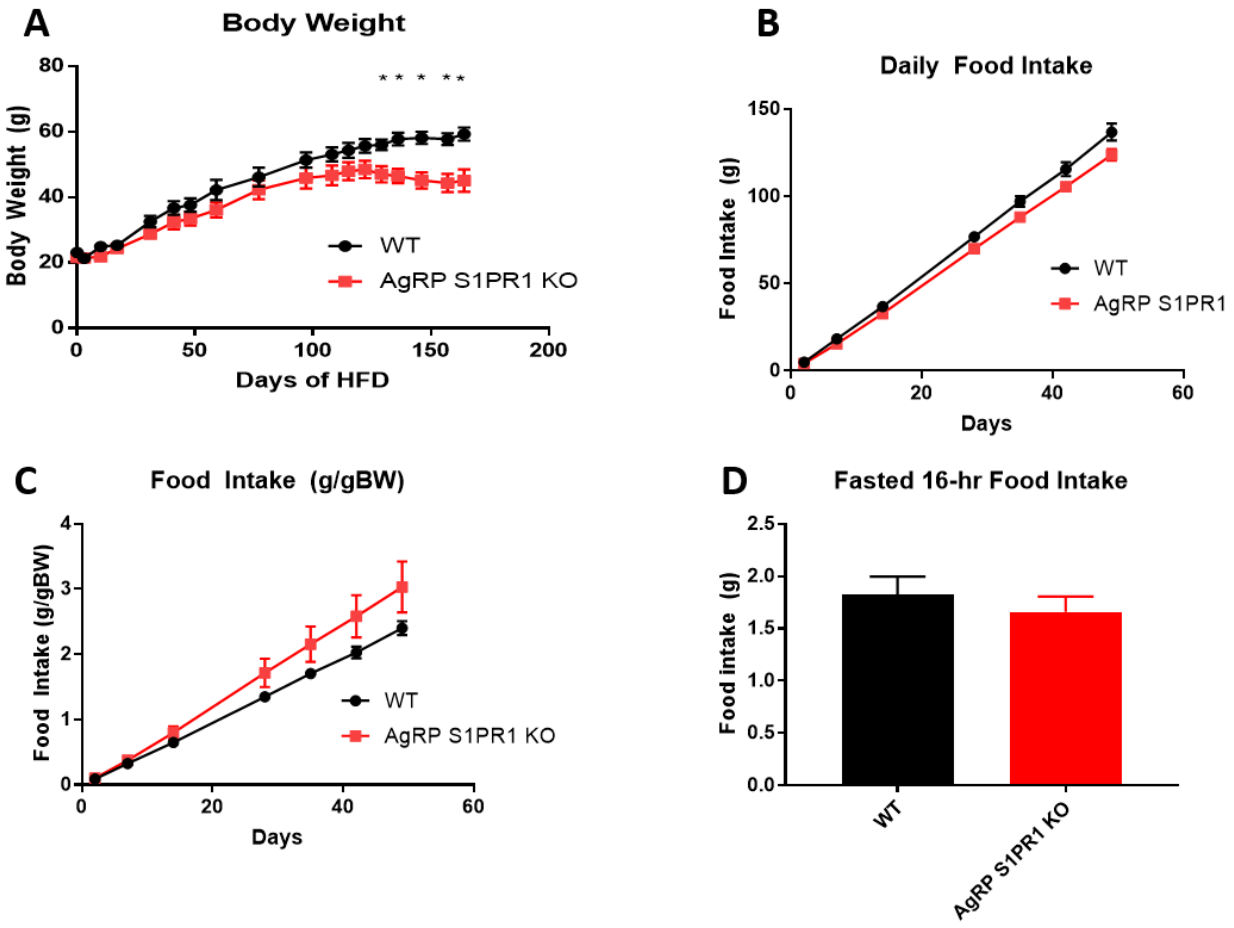

Figure 4.4: Ablation of S1PR1 in AgRP neurons decreases HFD-induced weight gain without altering food intake. WT and AgRP S1PR1^{KO} animals were fasted overnight and injected with tamoxifen (150 µg/kg) five times (with multiple days of rest between tamoxifen injections). After the induction of S1PR1 ablation, animals were provided HFD and body weights were monitored (A). Following the divergence of body weight, mice were single housed, and food intake was measured (B&C). After a 24-hour fast, mice were provided food for 16 hours and food intake was measured (D). n = 6 per group, * $p < 0.05$.

Figure 4.5

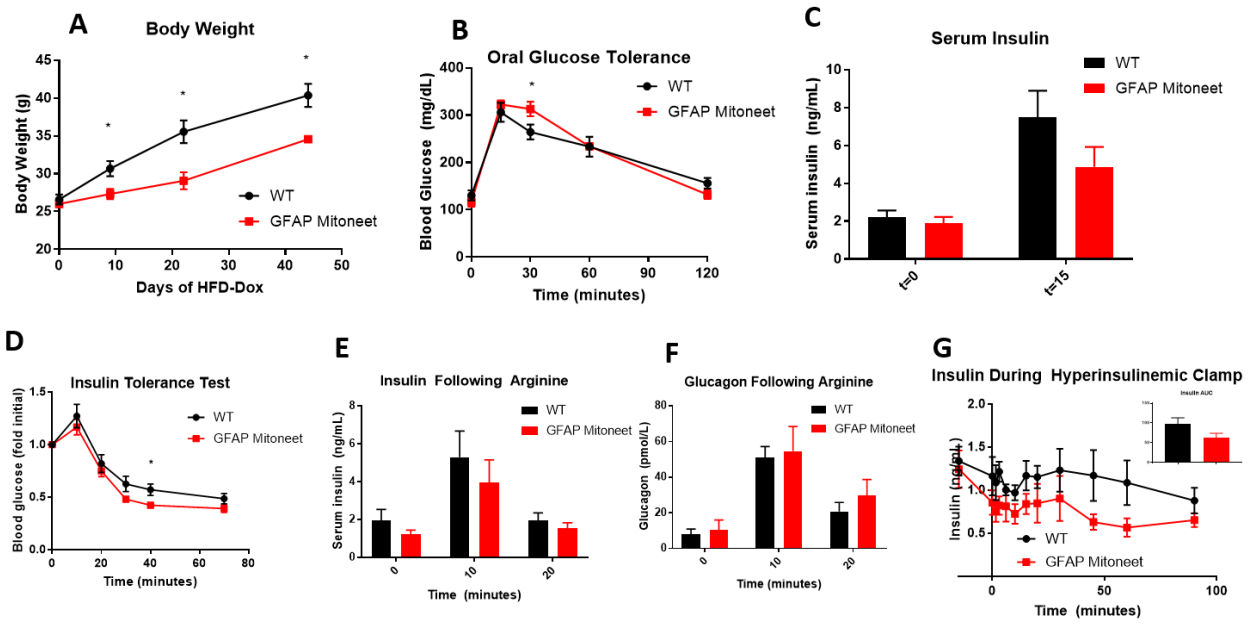

<u>Figure 4.5:</u> Overexpression of mitoNEET in astrocytes reduces body weight gain and decreases glucose tolerance due to decreased insulin secretion. WT and GFAP-mitoNEET mice were placed on HFD-dox and body weights were monitored for 6 weeks (A). Glucose tolerance (B) and glucose-stimulated insulin secretion (C) were assayed after 2.5 weeks of HFD-dox. Insulin tolerance was also assayed following high fat feeding (D). Insulin (E) and glucagon (F) were measured following an intraperitoneal injection of arginine (2 g/kg). Finally, insulin was measured periodically during a hyperglycemic clamp (G). $n \geq 3$ per group, $p < 0.05$.

Figure 4.6

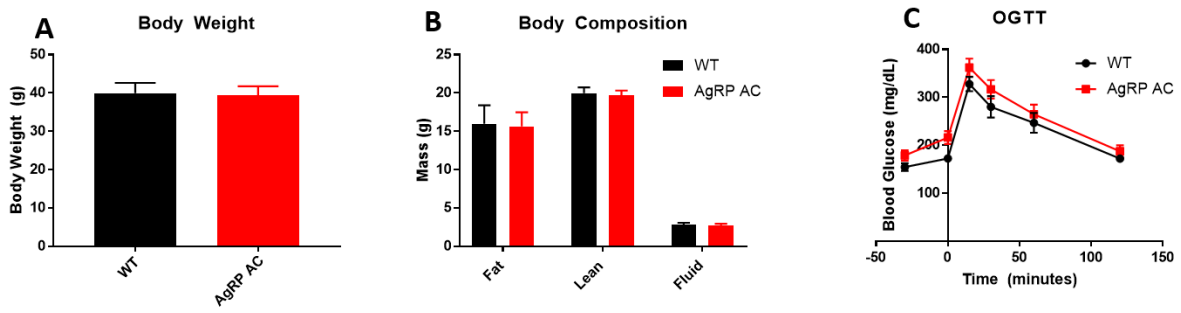

<u>Figure 4.6:</u> Overexpression of acid ceramidase in AgRP neurons does not alter body weight, body composition or glucose tolerance. WT and AgRP AC mice were provided HFD-dox, and body weight (A), body composition (B) and oral glucose tolerance (C) were assayed. n = 5-7 per group.

Figure 4.7

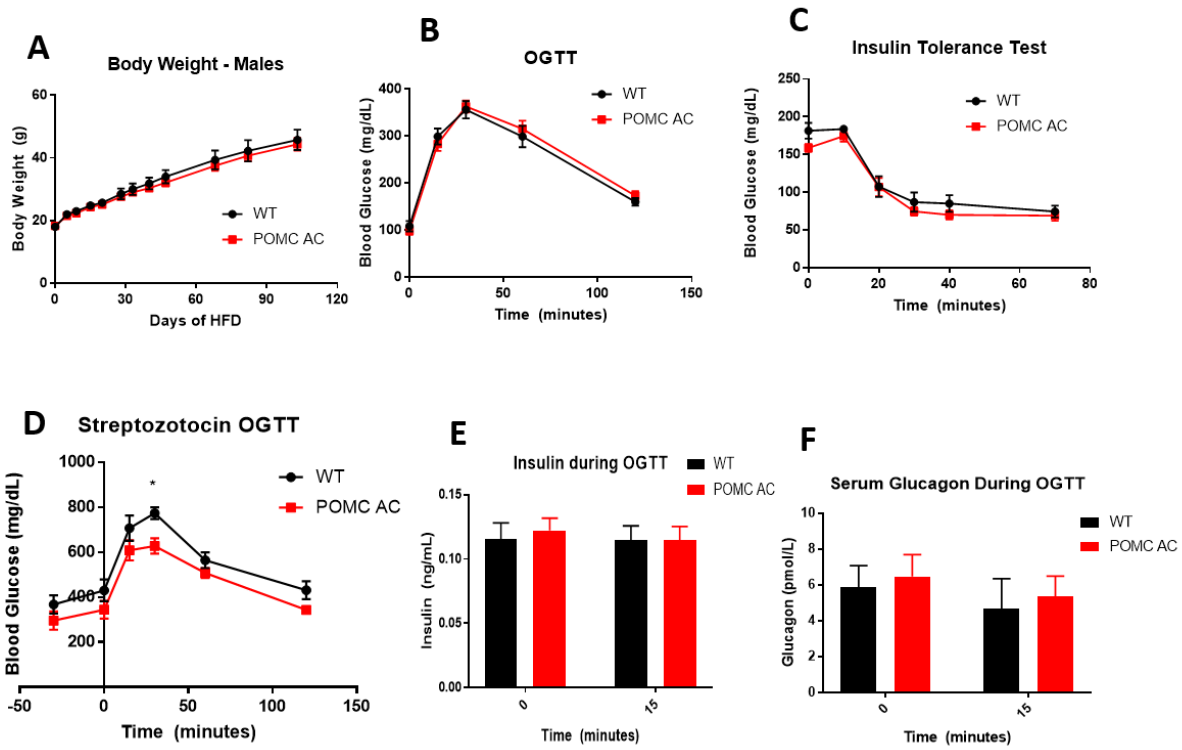

<u>Figure 4.7:</u> Overexpression of acid ceramidase in POMC neurons of male mice does not alter HFD-induced body weight gain or glucose intolerance, but confers minor protection to streptozotocin induced diabetes. WT and POMC AC mice were provided HFD-dox and body weight was monitored (A). Oral glucose tolerance (B) and insulin tolerance (C) were assayed at least 6 weeks following the beginning of HFD feeding. Streptozotocin (100 µg/kg) was injected in fasted animals twice, and mice were provided dox chow after one week. WT and POMC AC mice were assayed for oral glucose tolerance (D), and neither serum insulin (E) nor glucagon (F) were altered during the OGTT. $n \geq 5$ per group, * $p < 0.05$.

Figure 4.8

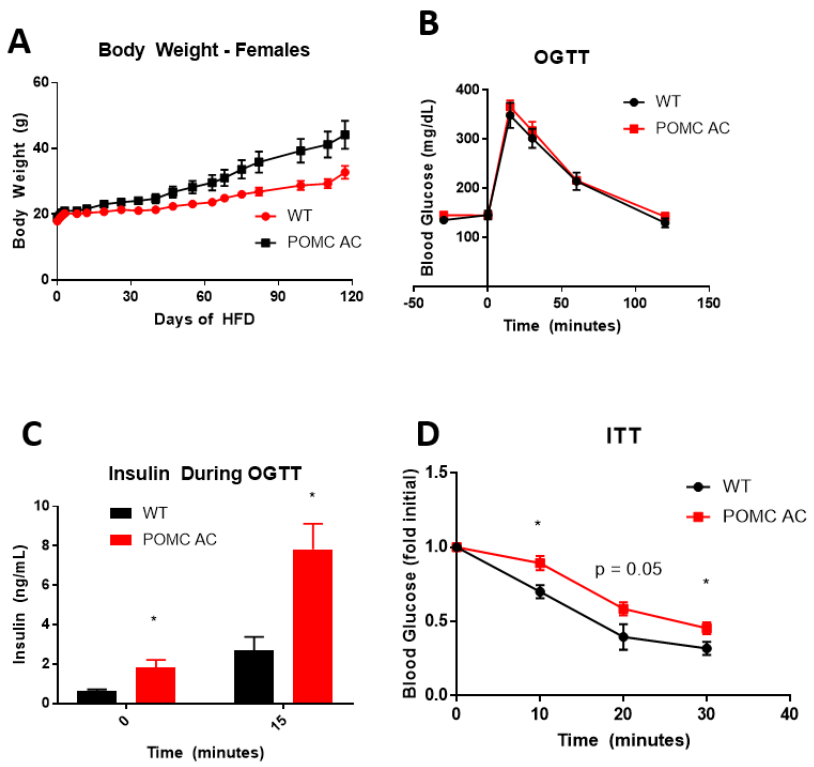

<u>Figure 4.8:</u> Overexpression of acid ceramidase in POMC neurons of female mice greatly increases diet-induced weight gain, while preserving glucose tolerance in the face of insulin resistance. WT and POMC AC female mice were provided HFD-dox for 4 months, and body weight was monitored (A). After 4 months of HFD feeding, animals were assayed for oral glucose tolerance (B) and glucose-stimulated insulin secretion (C). Insulin tolerance was then assayed (D). n = 5-9 per group, * $p < 0.05$.

Figure 4.9

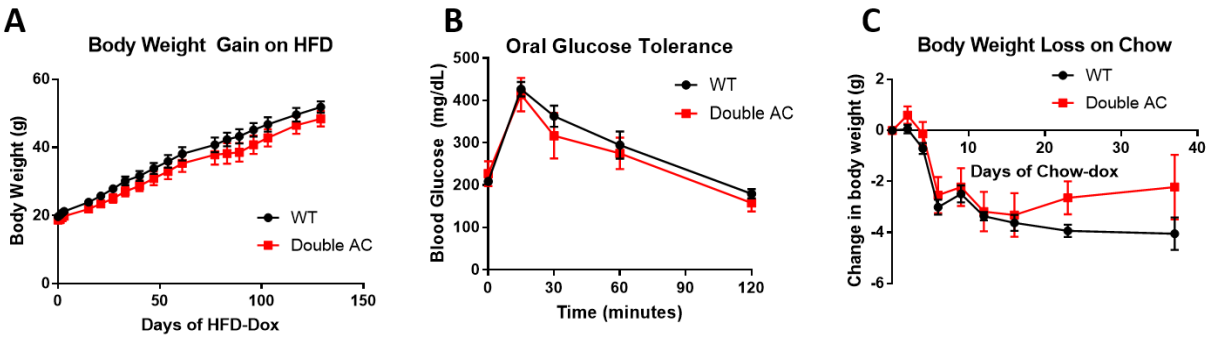

<u>Figure 4.9:</u> Overexpression of acid ceramidase in POMC and AgRP neurons of male mice does not alter HFD-induced body weight gain or glucose intolerance. WT and Double POMC/AgRP AC mice were provided HFD-dox for 4 months and body weight was monitored (A). After 4 months of HFD-dox, oral glucose tolerance was assayed (B). Following measurements of glucose tolerance, animals were switched to dox-chow from HFD and body weight was monitored (C).

References

1. Flegal, K.M., et al., *Prevalence of obesity and trends in the distribution of body mass index among US adults, 1999-2010.* Jama, 2012. **307**(5): p. 491-497.
2. Adams, K.F., et al., *Overweight, obesity, and mortality in a large prospective cohort of persons 50 to 71 years old.* New England Journal of Medicine, 2006. **355**(8): p. 763-778.
3. Lavie, C.J., R.V. Milani, and H.O. Ventura, *Obesity and cardiovascular disease.* Journal of the American College of Cardiology, 2009. **53**(21): p. 1925-1932.
4. Kahn, S.E., R.L. Hull, and K.M. Utzschneider, *Mechanisms linking obesity to insulin resistance and type 2 diabetes.* Nature, 2006. **444**(7121): p. 840.
5. Unger, R.H., et al., *Lipid homeostasis, lipotoxicity and the metabolic syndrome.* Biochimica et Biophysica Acta (BBA)-Molecular and Cell Biology of Lipids, 2010. **1801**(3): p. 209-214.
6. Samuel, V.T. and G.I. Shulman, *Mechanisms for insulin resistance: common threads and missing links.* Cell, 2012. **148**(5): p. 852-871.
7. Chavez, J.A. and S.A. Summers, *A ceramide-centric view of insulin resistance.* Cell metabolism, 2012. **15**(5): p. 585-594.
8. Miyake, Y., et al., *Serine palmitoyltransferase is the primary target of a sphingosine-like immunosuppressant, ISP-1/myriocin.* Biochemical and biophysical research communications, 1995. **211**(2): p. 396-403.
9. Ussher, J.R., et al., *Inhibition of de novo ceramide synthesis reverses diet-induced insulin resistance and enhances whole-body oxygen consumption.* Diabetes, 2010. **59**(10): p. 2453-64.
10. Holland, W.L., et al., *Inhibition of ceramide synthesis ameliorates glucocorticoid-, saturated-fat-, and obesity-induced insulin resistance.* Cell metabolism, 2007. **5**(3): p. 167-179.
11. Boini, K.M., et al., *Role of sphingolipid mediator ceramide in obesity and renal injury in mice fed a high-fat diet.* Journal of Pharmacology and Experimental Therapeutics, 2010. **334**(3): p. 839-846.
12. Chaurasia, B., et al., *Adipocyte ceramides regulate subcutaneous adipose browning, inflammation, and metabolism.* Cell metabolism, 2016. **24**(6): p. 820-834.
13. Yang, G., et al., *Central role of ceramide biosynthesis in body weight regulation, energy metabolism, and the metabolic syndrome.* Am J Physiol Endocrinol Metab, 2009. **297**(1): p. E211-24.
14. Zhang, Q.J., et al., *Ceramide mediates vascular dysfunction in diet-induced obesity by PP2A-mediated dephosphorylation of the eNOS-Akt complex.* Diabetes, 2012. **61**(7): p. 1848-59.
15. Glaros, E.N., et al., *Myriocin slows the progression of established atherosclerotic lesions in apolipoprotein E gene knockout mice.* Journal of lipid research, 2008. **49**(2): p. 324-331.
16. Aerts, J.M., et al., *Pharmacological inhibition of glucosylceramide synthase enhances insulin sensitivity.* Diabetes, 2007. **56**(5): p. 1341-1349.
17. Zhao, H., et al., *Inhibiting glycosphingolipid synthesis improves glycemic control and insulin sensitivity in animal models of type 2 diabetes.* Diabetes, 2007. **56**(5): p. 1210-1218.
18. Ashe, K.M., et al., *Iminosugar-based inhibitors of glucosylceramide synthase increase brain glycosphingolipids and survival in a mouse model of Sandhoff disease.* PLoS One, 2011. **6**(6): p. e21758.
19. Yew, N.S., et al., *Increased hepatic insulin action in diet-induced obese mice following inhibition of glucosylceramide synthase.* PLoS one, 2010. **5**(6): p. e11239.
20. Bijl, N., et al., *Modulation of glycosphingolipid metabolism significantly improves hepatic insulin sensitivity and reverses hepatic steatosis in mice.* Hepatology, 2009. **50**(5): p. 1431-1441.
21. van Eijk, M., et al., *Reducing glycosphingolipid content in adipose tissue of obese mice restores insulin sensitivity, adipogenesis and reduces inflammation.* PLoS One, 2009. **4**(3): p. e4723.

22. Bietrix, F., et al., *Inhibition of glycosphingolipid synthesis induces a profound reduction of plasma cholesterol and inhibits atherosclerosis development in APOE* 3 Leiden and low-density lipoprotein receptor−/− mice.* Arteriosclerosis, thrombosis, and vascular biology, 2010. **30**(5): p. 931-937.
23. Lombardo, E., et al., *Correction of liver steatosis by a hydrophobic iminosugar modulating glycosphingolipids metabolism.* PLoS One, 2012. **7**(10): p. e38520.
24. Langeveld, M., et al., *Treatment of genetically obese mice with the iminosugar N-(5-adamantane-1-yl-methoxy-pentyl)-deoxynojirimycin reduces body weight by decreasing food intake and increasing fat oxidation.* Metabolism, 2012. **61**(1): p. 99-107.
25. Lee, S.-Y., et al., *Adipocyte-Specific Deficiency of de novo Sphingolipid Biosynthesis Leads to Lipodystrophy and Insulin Resistance.* Diabetes, 2017: p. db161232.
26. Alexaki, A., et al., *De novo sphingolipid biosynthesis is required for adipocyte survival and metabolic homeostasis.* Journal of Biological Chemistry, 2017. **292**(9): p. 3929-3939.
27. Li, Z., et al., *Reducing plasma membrane sphingomyelin increases insulin sensitivity.* Molecular and cellular biology, 2011. **31**(20): p. 4205-4218.
28. Grösch, S., S. Schiffmann, and G. Geisslinger, *Chain length-specific properties of ceramides.* Progress in lipid research, 2012. **51**(1): p. 50-62.
29. Turpin, S.M., et al., *Obesity-induced CerS6-dependent C16:0 ceramide production promotes weight gain and glucose intolerance.* Cell Metab, 2014. **20**(4): p. 678-86.
30. Gosejacob, D., et al., *Ceramide synthase 5 is essential to maintain C16: 0-ceramide pools and contributes to the development of diet-induced obesity.* Journal of Biological Chemistry, 2016. **291**(13): p. 6989-7003.
31. Raichur, S., et al., *CerS2 haploinsufficiency inhibits β-oxidation and confers susceptibility to diet-induced steatohepatitis and insulin resistance.* Cell metabolism, 2014. **20**(4): p. 687-695.
32. Mitsutake, S., et al., *Ceramide kinase deficiency improves diet-induced obesity and insulin resistance.* FEBS letters, 2012. **586**(9): p. 1300-1305.
33. Holland, W.L., et al., *Receptor-mediated activation of ceramidase activity initiates the pleiotropic actions of adiponectin.* Nature medicine, 2011. **17**(1): p. 55-63.
34. Vasiliauskaité-Brooks, I., et al., *Structural insights into adiponectin receptors suggest ceramidase activity.* Nature, 2017. **544**(7648): p. 120.
35. Holland, W.L., et al., *Inducible overexpression of adiponectin receptors highlight the roles of adiponectin-induced ceramidase signaling in lipid and glucose homeostasis.* Molecular metabolism, 2017. **6**(3): p. 267-275.
36. Tanabe, H., et al., *Crystal structures of the human adiponectin receptors.* Nature, 2015. **520**(7547): p. 312.
37. Personal communication, AL Ghaben & PE Scherer
38. Xia, J.Y., et al., *Targeted induction of ceramide degradation leads to improved systemic metabolism and reduced hepatic steatosis.* Cell metabolism, 2015. **22**(2): p. 266-278.
39. Personal communication, TS Morley & PE Scherer
40. Unpublished data, AX Sharma & WL Holland.
41. Boon, J., et al., *Ceramides contained in LDL are elevated in type 2 diabetes and promote inflammation and skeletal muscle insulin resistance.* Diabetes, 2013. **62**(2): p. 401-410.
42. González-García, I., et al., *Hypothalamic lipids: key regulators of whole body energy balance.* Neuroendocrinology, 2017. **104**(4): p. 398-411.
43. Borg, M.L., et al., *Consumption of a high-fat diet, but not regular endurance exercise training, regulates hypothalamic lipid accumulation in mice.* The Journal of physiology, 2012. **590**(17): p. 4377-4389.

44. Holland, W.L., et al., *Lipid-induced insulin resistance mediated by the proinflammatory receptor TLR4 requires saturated fatty acid–induced ceramide biosynthesis in mice.* The Journal of clinical investigation, 2011. **121**(5): p. 1858.
45. Gao, S., et al., *Important roles of brain-specific carnitine palmitoyltransferase and ceramide metabolism in leptin hypothalamic control of feeding.* Proc Natl Acad Sci U S A, 2011. **108**(23): p. 9691-6.
46. Ramirez, S., et al., *Hypothalamic ceramide levels regulated by CPT1C mediate the orexigenic effect of ghrelin.* Diabetes, 2013. **62**(7): p. 2329-37.
47. Contreras, C., et al., *Central Ceramide-Induced Hypothalamic Lipotoxicity and ER Stress Regulate Energy Balance.* Cell Rep, 2014. **9**(1): p. 366-77.
48. Martínez-Sánchez, N., et al., *Hypothalamic AMPK-ER Stress-JNK1 Axis Mediates the Central Actions of Thyroid Hormones on Energy Balance.* Cell Metabolism, 2017. **26**(1): p. 212-229. e12.
49. Hargrave, S.L., S. Jones, and T.L. Davidson, *The outward spiral: a vicious cycle model of obesity and cognitive dysfunction.* Current opinion in behavioral sciences, 2016. **9**: p. 40-46.
50. Picard, A., et al., *Hippocampal lipoprotein lipase regulates energy balance in rodents.* Molecular metabolism, 2014. **3**(2): p. 167-176.
51. Nordström, V., et al., *Neuronal expression of glucosylceramide synthase in central nervous system regulates body weight and energy homeostasis.* PLoS biology, 2013. **11**(3): p. e1001506.
52. Herzer, S., et al., *Fasting-induced lipolysis and hypothalamic insulin signaling are regulated by neuronal glucosylceramide synthase.* Diabetes, 2015. **64**(10): p. 3363-3376.
53. Bourbon, N.A., L. Sandirasegarane, and M. Kester, *Ceramide-induced Inhibition of Akt Is Mediated through Protein Kinase Cζ IMPLICATIONS FOR GROWTH ARREST.* Journal of Biological Chemistry, 2002. **277**(5): p. 3286-3292.
54. Teruel, T., R. Hernandez, and M. Lorenzo, *Ceramide mediates insulin resistance by tumor necrosis factor-α in brown adipocytes by maintaining Akt in an inactive dephosphorylated state.* Diabetes, 2001. **50**(11): p. 2563-2571.
55. Klöckener, T., et al., *High-fat feeding promotes obesity via insulin receptor/PI3K-dependent inhibition of SF-1 VMH neurons.* Nature neuroscience, 2011. **14**(7): p. 911-918.
56. Brüning, J.C., et al., *Role of brain insulin receptor in control of body weight and reproduction.* Science, 2000. **289**(5487): p. 2122-2125.
57. Lin, H.V., et al., *Divergent regulation of energy expenditure and hepatic glucose production by insulin receptor in agouti-related protein and POMC neurons.* Diabetes, 2010. **59**(2): p. 337-346.
58. Hill, J.W., et al., *Direct insulin and leptin action on pro-opiomelanocortin neurons is required for normal glucose homeostasis and fertility.* Cell metabolism, 2010. **11**(4): p. 286-297.
59. Könner, A.C., et al., *Insulin action in AgRP-expressing neurons is required for suppression of hepatic glucose production.* Cell metabolism, 2007. **5**(6): p. 438-449.
60. Montague, C.T., et al., *Congenital leptin deficiency is associated with severe early-onset obesity in humans.* Nature, 1997. **387**(6636): p. 903-908.
61. Zhang, Y., et al., *Positional cloning of the mouse obese gene and its human homologue.* Nature, 1994. **372**(6505): p. 425-432.
62. Halaas, J.L., et al., *Weight-reducing effects of the plasma protein encoded by the obese gene.* Science-AAAS-Weekly Paper Edition, 1995. **269**(5223): p. 543-545.
63. Hill, J.W., et al., *Acute effects of leptin require PI3K signaling in hypothalamic proopiomelanocortin neurons in mice.* The Journal of clinical investigation, 2008. **118**(5): p. 1796.
64. Gulbins, E., et al., *A central role for the acid sphingomyelinase/ceramide system in neurogenesis and major depression.* Journal of neurochemistry, 2015. **134**(2): p. 183-192.
65. Kokoeva, M.V., H. Yin, and J.S. Flier, *Neurogenesis in the hypothalamus of adult mice: potential role in energy balance.* Science, 2005. **310**(5748): p. 679-683.

66. Pierce, A.A. and A.W. Xu, *De novo neurogenesis in adult hypothalamus as a compensatory mechanism to regulate energy balance.* Journal of Neuroscience, 2010. **30**(2): p. 723-730.
67. Colombaioni, L. and M. Garcia-Gil, *Sphingolipid metabolites in neural signalling and function.* Brain Research Reviews, 2004. **46**(3): p. 328-355.
68. Elson, A.E.T. and R.B. Simerly, *Developmental Specification of Metabolic Circuitry.* Front Neuroendocrinol, 2015. **39**: p. 38-51.
69. Mitsutake, S., et al., *The generation and behavioral analysis of ceramide kinase-null mice, indicating a function in cerebellar Purkinje cells.* Biochemical and biophysical research communications, 2007. **363**(3): p. 519-524.
70. Yamashita, T., et al., *Conditional LoxP-flanked glucosylceramide synthase allele controlling glycosphingolipid synthesis.* Genesis, 2005. **43**(4): p. 175-80.
71. Bosio, A., E. Binczek, and W. Stoffel, *Functional breakdown of the lipid bilayer of the myelin membrane in central and peripheral nervous system by disrupted galactocerebroside synthesis.* Proceedings of the National Academy of Sciences, 1996. **93**(23): p. 13280-13285.
72. Brady, R.O., et al., *The metabolism of sphingomyelin. II. Evidence of an enzymatic deficiency in Niemann-Pick diseae.* Proceedings of the National Academy of Sciences, 1966. **55**(2): p. 366-369.
73. Kitatani, K., J. Idkowiak-Baldys, and Y.A. Hannun, *The sphingolipid salvage pathway in ceramide metabolism and signaling.* Cellular signalling, 2008. **20**(6): p. 1010-1018.
74. Rodgers, R.J., M.H. Tschöp, and J.P. Wilding, *Anti-obesity drugs: past, present and future.* Disease models & mechanisms, 2012. **5**(5): p. 621-626.
75. Elmquist, J.K., C.F. Elias, and C.B. Saper, *From lesions to leptin: hypothalamic control of food intake and body weight.* Neuron, 1999. **22**(2): p. 221-232.
76. Coll, A.P. and G.S. Yeo, *The hypothalamus and metabolism: integrating signals to control energy and glucose homeostasis.* Current opinion in pharmacology, 2013. **13**(6): p. 970-976.
77. Coppari, R., *Hypothalamic Neurones Governing Glucose Homeostasis.* Journal of neuroendocrinology, 2015. **27**(6): p. 399-405.
78. Choi, Y.-H., et al., *Revisiting the ventral medial nucleus of the hypothalamus: the roles of SF-1 neurons in energy homeostasis.* Frontiers in neuroscience, 2013. **7**.
79. Borg, M.A., et al., *Local ventromedial hypothalamus glucose perfusion blocks counterregulation during systemic hypoglycemia in awake rats.* Journal of Clinical Investigation, 1997. **99**(2): p. 361.
80. Borg, W.P., et al., *Ventromedial hypothalamic lesions in rats suppress counterregulatory responses to hypoglycemia.* Journal of Clinical Investigation, 1994. **93**(4): p. 1677.
81. Tong, Q., et al., *Synaptic glutamate release by ventromedial hypothalamic neurons is part of the neurocircuitry that prevents hypoglycemia.* Cell metabolism, 2007. **5**(5): p. 383-393.
82. Kamitakahara, A., B. Xu, and R. Simerly, *Ventromedial hypothalamic expression of Bdnf is required to establish normal patterns of afferent GABAergic connectivity and responses to hypoglycemia.* Molecular metabolism, 2016. **5**(2): p. 91-101.
83. Ramadori, G., et al., *SIRT1 deacetylase in SF1 neurons protects against metabolic imbalance.* Cell metabolism, 2011. **14**(3): p. 301-312.
84. Fujikawa, T., et al., *SF-1 expression in the hypothalamus is required for beneficial metabolic effects of exercise.* Elife, 2016. **5**: p. e18206.
85. Kim, K.W., et al., *FOXO1 in the ventromedial hypothalamus regulates energy balance.* The Journal of clinical investigation, 2012. **122**(7): p. 2578.
86. Zhang, R., et al., *Selective inactivation of Socs3 in SF1 neurons improves glucose homeostasis without affecting body weight.* Endocrinology, 2008. **149**(11): p. 5654-5661.
87. Dhillon, H., et al., *Leptin directly activates SF1 neurons in the VMH, and this action by leptin is required for normal body-weight homeostasis.* Neuron, 2006. **49**(2): p. 191-203.

88. Gault, C.R., L.M. Obeid, and Y.A. Hannun, *An overview of sphingolipid metabolism: from synthesis to breakdown*, in *Sphingolipids as Signaling and Regulatory Molecules*. 2010, Springer. p. 1-23.
89. Belteki, G., et al., *Conditional and inducible transgene expression in mice through the combinatorial use of Cre-mediated recombination and tetracycline induction.* Nucleic acids research, 2005. **33**(5): p. e51-e51.
90. Stallings, N.R., et al., *Development of a transgenic green fluorescent protein lineage marker for steroidogenic factor 1.* Molecular Endocrinology, 2002. **16**(10): p. 2360-2370.
91. Sun, J., et al., *Adiponectin potentiates the acute effects of leptin in arcuate Pomc neurons.* Molecular metabolism, 2016. **5**(10): p. 882-891.
92. Kusminski, C.M., et al., *MitoNEET-driven alterations in adipocyte mitochondrial activity reveal a crucial adaptive process that preserves insulin sensitivity in obesity.* Nature medicine, 2012. **18**(10): p. 1539-1549.
93. Longuet, C., et al., *The glucagon receptor is required for the adaptive metabolic response to fasting.* Cell metabolism, 2008. **8**(5): p. 359-371.
94. Duggan, J. and D. Booth, *Obesity, overeating, and rapid gastric emptying in rats with ventromedial hypothalamic lesions.* Science, 1986. **231**: p. 609-612.
95. Douglass, J.D., M.D. Dorfman, and J.P. Thaler, *Glia: silent partners in energy homeostasis and obesity pathogenesis.* Diabetologia, 2017: p. 1-11.
96. Ganat, Y.M., et al., *Early postnatal astroglial cells produce multilineage precursors and neural stem cells in vivo.* Journal of Neuroscience, 2006. **26**(33): p. 8609-8621.
97. Zhuo, L., et al., *hGFAP-cre transgenic mice for manipulation of glial and neuronal function in vivo.* genesis, 2001. **31**(2): p. 85-94.
98. Berglund, E.D., et al., *Serotonin 2C receptors in pro-opiomelanocortin neurons regulate energy and glucose homeostasis.* The Journal of clinical investigation, 2013. **123**(12): p. 5061-5070.
99. Wang, Q., et al., *Arcuate AgRP neurons mediate orexigenic and glucoregulatory actions of ghrelin.* Molecular metabolism, 2014. **3**(1): p. 64-72.
100. Allende, M.L., T. Yamashita, and R.L. Proia, *G-protein-coupled receptor S1P1 acts within endothelial cells to regulate vascular maturation.* Blood, 2003. **102**(10): p. 3665-3667.
101. Tong, Q., et al., *Synaptic release of GABA by AgRP neurons is required for normal regulation of energy balance.* Nature neuroscience, 2008. **11**(9): p. 998.
102. Balthasar, N., et al., *Leptin receptor signaling in POMC neurons is required for normal body weight homeostasis.* Neuron, 2004. **42**(6): p. 983-991.
103. Buckman, L.B., et al., *Evidence for a novel functional role of astrocytes in the acute homeostatic response to high-fat diet intake in mice.* Molecular metabolism, 2015. **4**(1): p. 58-63.
104. Nagatsuma, K., et al., *Lecithin: retinol acyltransferase protein is distributed in both hepatic stellate cells and endothelial cells of normal rodent and human liver.* Liver International, 2009. **29**(1): p. 47-54.
105. Williams, K.W. and J.K. Elmquist, *From neuroanatomy to behavior: central integration of peripheral signals regulating feeding behavior.* Nature neuroscience, 2012. **15**(10): p. 1350.
106. Silva, V.R., et al., *Hypothalamic S1P/S1PR1 axis controls energy homeostasis.* Nature communications, 2014. **5**: p. 4859.
107. Wang, H., et al., *Deficiency of lipoprotein lipase in neurons modifies the regulation of energy balance and leads to obesity.* Cell metabolism, 2011. **13**(1): p. 105-113.
108. Wiley, S.E., et al., *MitoNEET is an iron-containing outer mitochondrial membrane protein that regulates oxidative capacity.* Proceedings of the National Academy of Sciences, 2007. **104**(13): p. 5318-5323.

109. García-Cáceres, C., et al., *Astrocytic insulin signaling couples brain glucose uptake with nutrient availability.* Cell, 2016. **166**(4): p. 867-880.
110. Morselli, E., et al., *Hypothalamic PGC-1α Protects Against High Fat Diet Exposure by Regulating ERα.* Cell reports, 2014. **9**(2): p. 633-645.

LIST OF TABLES

LIST OF FIGURES

Chapter 2

Chapter 3

LIST OF FIGURES CONTINUED

Chapter 4